INTERNATIONAL JOURNAL FOR NUMERICAL METHODS IN FLUIDS, VOL. 3, 445–479 (1983)

A FRONTAL METHOD BASED SOLUTION OF THE QUASI-THREE-DIMENSIONAL FINITE ELEMENT MODEL FOR INTERCONNECTED AQUIFER SYSTEMS. STEADY AND UNSTEADY EQUATIONS, WITH THE E.N.S. METHOD FOR FLUID MASS BALANCE EVALUATION

L. SARTORI AND G. PEVERIERI

Aquater S.p.A., S. Lorenzo in Campo (PS), Italy

SUMMARY

The quasi-three-dimensional equations controlling the groundwater flow in heterogeneous and interconnected aquifer systems are discretized by finite elements, considering also the aquifer branching. A new method for fluid mass balance evaluation based on the equivalent nodal source (E.N.S.) concept allows one to express the balance in conservative terms, and interpret finite element equations as nodal balance equations. The solution of the system is based on the frontal method. Use of substructures limits the frontal increase in correspondence to the aquifer branching. In the steady state, the frontal method is integrated with an iterative solution technique to eliminate the frontal increase caused by the presence of aquitards. It converges very rapidly, using a forcing technique with an automatic parameter definition. In the unsteady case the same scope is achieved using a predictor–corrector procedure which employs the Crank–Nicolson method in the corrector phase.

This very stable procedure permits use of fairly long time-steps and concerns the case of source terms depending on piezometry (problem of interaction between water table and river). This method has been tested with several fairly complex cases.

KEY WORDS Finite Element Quasi-three-dimensional Interconnected Aquifer Systems Fluid Mass Balance Iterated Frontal Method Predictor–Corrector Method

INTRODUCTION

The quasi-three-dimensional equations governing the groundwater flow in regional aquifer systems are the most suitable to describe the physical system. In fact, unlike the two-dimensional equations, they allow the proper representation of aquifers lying on superimposed levels, hydraulically connected by means of interbedded aquitards. In addition this model takes into consideration the aquifer branching. In fact it is the only model that correctly outlines the phenomenon at a regional scale, inasmuch as the three-dimensional model, which theoretically better represents the ground water trend, in this context could not be used for practical purposes.

The regional aquifers are characterized by surface dimensions much larger than the thickness. To avoid ill-condition in the solution of the linear system, the mesh's dimensions should all be of the same magnitude order. In the three-dimensional case, this

0271–2091/83/050445–35$03.50

Received 22 December 1981
Revised 23 July 1982

would imply an excessive number of meshes, also for problems of limited areal extension.

Neuman and Witherspoon[1] pointed out that the solution of a quasi-three-dimensional model is near to the three-dimensional one, in the case in which the permeability contrast between aquifers and aquitards is of several orders of magnitude (as occurs in reality). Recently, several authors have used various methods for the discretization and numerical solution of these equations. Mathematical models for aquifer systems requires a different degree of detail for different areas of the aquifer system. This implies use of a method which allows a discretization with meshes of different widths, in the various network areas. Fujinawa[2,3] and Chorley and Frind[4] describe the finite element discretization of the problem in the hypothesis of overlying aquifers with interbedded aquitards.

The practical value of the above mentioned methods is nevertheless limited owing to the lack of adequate solutions for the aquifer branching problem and for fluid mass balance evaluation. The solution to these problems is given in this paper. Moreover the numerical methods developed fulfil all the requirements for their industrial application (capability to solve a large linear system without any problem of convergence and stability, with limited use of CPU time).

QUASI-THREE-DIMENSIONAL MODEL EQUATIONS

In the quasi-three-dimensional model the aquifer system is composed of aquifers and aquitards. The latter are made up of semipermeable layers which separate superimposed aquifer zones. The aquifers could present branching as shown in Figure 1.

Water flow has a horizontal course on the aquifers and is here governed by two-dimensional equations. It has a vertical course on aquitards, and is governed by one-dimensional equations.

The quasi-three-dimensional model originates from coupling two-dimensional equations for aquifers with the one-dimensional equations for aquitards. The following equation describes the two-dimensional water flow for the aquifers:

$$\frac{\partial}{\partial x}\left(T\frac{\partial h}{\partial x}\right)+\frac{\partial}{\partial y}\left(T\frac{\partial h}{\partial y}\right)=L_2-L_1+Q+S\frac{\partial h}{\partial t} \tag{1}$$

where

T = transmissivity (fixed for confined aquifers, linearly dependent on the piezometry for phreatic aquifers)

L_2 and L_1 = top and bottom leakage terms

Q = source term

S = storage coefficient for confined aquifers and effective porosity for phreatic aquifers.

h = average aquifer piezometry (averaged along aquifer thickness).

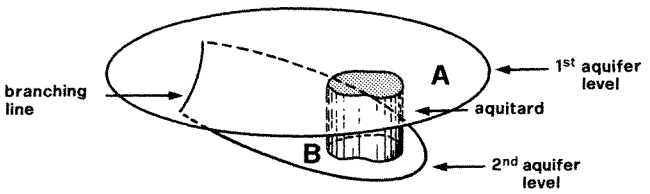

Figure 1. Multilayered aquifer system

The following one-dimensional equation is used for the aquitards:

$$\frac{\partial}{\partial z}\left(K\frac{\partial h^*}{\partial z}\right)=S_s\frac{\partial h^*}{\partial t} \tag{2}$$

where

K = vertical permeability of aquitard
S_s = specific storage coefficient
h^* = piezometry along aquitard thickness

The conditions that should be applied to the aquifer boundary are of the Dirichlet type:

$$h=h_0, \quad \text{on } \Gamma_1 \tag{3}$$

and of Neumann type:

$$-T\frac{\partial h}{\partial n}=\varphi_0 \quad \text{on } \Gamma_2 \tag{4}$$

where $\Gamma=\Gamma_1+\Gamma_2$ is the aquifer boundary. Along the aquifer branching lines, the piezometry continuity conditions are:

$$h_1=h_2=h_3 \tag{5}$$

and the flow conservation:

$$\varphi_1+\varphi_2+\varphi_3=0 \tag{6}$$

$$\varphi=-T\frac{\partial h}{\partial n} \tag{7}$$

The derivative $\partial h/\partial n$ should be calculated along the normal at the branching line. Coupling of the aquifer two-dimensional equations (1) with the aquitard one-dimensional equations (2) takes place through leakage terms:

$$L_2=-K\left(\frac{\partial h^*}{\partial z}\right)_{z=z_T}; \qquad L_1=-K\left(\frac{\partial h^*}{\partial z}\right)_{z=z_B} \tag{8}$$

(z_T and z_B are the quotas at top and bottom of the aquitard respectively)[2] and identifying the piezometry of the aquitard with that of the aquifer in correspondence to separation surface at top and bottom of the aquitard:

$$h^*(t, x, y, z_T)=h_T(t, x, y); \quad h^*(t, x, y, z_B)=h_B(t, x, y) \tag{9}$$

Finally, the initial conditions at aquifers and aquitards should be added.

Finite element discretization and formulation of the E.N.S. method for the fluid mass balances

The Galerkin method is applied for the finite element discretization, with linear shape functions both for aquifers and aquitards. Triangular elements are used for aquifers. On the aquitards the one-dimensional finite elements, which connect two nodes located along the same vertical, are all the same length and together form an aquitard macroelement.

Figure 2 illustrates this discretization, pointing out the branching line treatment and the

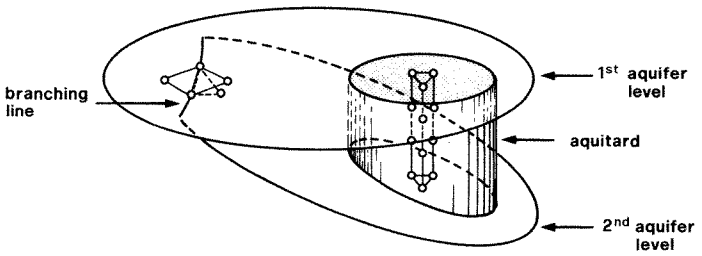

Figure 2. Finite element discretization of a multilayered aquifer

connections between aquifers and aquitards. By applying the Galerkin method to equation (2) valid for aquitards, we obtain the differential equation system:

$$\mathbf{C}^*\dot{\mathbf{h}}^* + \mathbf{A}^*\mathbf{h}^* = \mathbf{b}^* \tag{10}$$

These equations concern only the nodes within aquitard macroelements, or the boundary nodes which are subject to imposed flow conditions. The right-hand terms of the system are all null except those related to nodes near those subject to imposed piezometry conditions, or subject to imposed flow conditions. For the latter, the right-hand term is:

$$b_i = -L \tag{11}$$

where L = imposed flow (or leakage) on the node.

The matrices included in system (10) are obtained by assembling similar matrices and right hand terms pertaining to generic elements of nodes i and j (i precedes j on the vertical). The matrices are:

$$\mathbf{A}^*_{l,m} = \frac{K}{\Delta z}\begin{bmatrix} 1 & -1 \\ -1 & 1 \end{bmatrix}; \qquad \mathbf{C}^*_{l,m} = \frac{S_s \Delta z}{6}\begin{bmatrix} 2 & 1 \\ 1 & 2 \end{bmatrix} \tag{12}$$

$l = i, j$; $m = i, j$; $\Delta z = (z_j - z_i)$.

The fluid mass balance can be estimated with the E.N.S. method for each element on the basis of the following four items:

F_i = imposed flow
F_c = flow deriving from contiguous elements
F_p = flow equivalent to imposed piezometry conditions
F_u = storage depletion

This balance concerns a column of aquitards of unit section which extends over the entire element thickness. The first item is present only if a node of the element is subject to imposed flow conditions. The second item is present in correspondence to each node which is not subject to imposed flow conditions nor to imposed piezometry conditions.

In order to define, on an element node, the flow deriving from contiguous elements, we will divide the macroelement into two parts A and B corresponding to node P_i (Figure 4). We will define in element (l) the flow deriving from element ($l+1$) through node P_i, as that flow which, when imposed on node P_i at part A of the macroelement, supposedly interrupted on P_i (see Figure 4), is able to reproduce on part A of the structure, the same piezometry obtained on the uninterrupted structure, as in Figure 3.

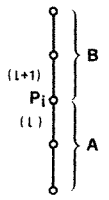

Figure 3. Non-interrupted macroelement

If we indicate the contributions to assembly system (10) of matrices deriving from part A of the macroelement using a_{is}^{A} and c_{is}^{A}, and those deriving from part B using a_{is}^{B} and c_{is}^{B}, in relation to node P_i:

$$\left.\begin{aligned} a_{is} &= a_{is}^{A} + a_{is}^{B} \\ c_{is} &= c_{is}^{A} + c_{is}^{B} \end{aligned}\right\} \tag{13}$$

The equation of system (10) related to node P_i (internal) could be written as follows:

$$\left.\begin{aligned} \sum a_{is}^{A} h_s^* + \sum c_{is}^{A} \dot{h}_s^* &= -L \\ -L = -\sum a_{is}^{B} h_s^* - \sum c_{is}^{B} \dot{h}_s^* \end{aligned}\right\} \tag{14}$$

The term L which appears in (14) represents, on the basis of the given definition, the flow originating from part B on part A through node P_i. In order to define the flow with these equations it is necessary to previously calculate the piezometry, thus solving system (10). In this case, for the evaluation of flow L it is convenient to use the first equation of system (14). This allows determination of flow deriving from part B on part A through node P_i, resorting only to part A data.

In particular, using only the matrices $A_{l,m}$, $C_{l,m}$ of an element, it is possible to define the incoming flow, through the nodes of the element.

$$F_{ci} = K\frac{h_j^* - h_i^*}{\Delta z} - \frac{S_s \Delta z}{6}(2\dot{h}_i^* + \dot{h}_j^*) \tag{15}$$

$$F_{cj} = -K\frac{h_j^* - h_i^*}{\Delta z} - \frac{S_s \Delta z}{6}(\dot{h}_i^* + 2\dot{h}_j^*) \tag{16}$$

In a similar manner, we could define the flow equivalent to the imposed piezometry conditions as the flow imposed on a node, instead of the imposed piezometry condition, able to reproduce the same piezometric values on the aquitard macroelement.

The same equations (15) and (16) can be obtained for the terms F_{pi} and F_{pj}. The last balance item, the flow which represents storage depletion in unsteady state, is given by the

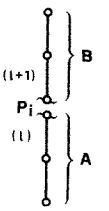

Figure 4. Interrupted macroelement

following:

$$F_i = \int_{z_i}^{z_j} S_s \dot{h}^*(z)\,dz = S_s \Delta z \frac{\dot{h}_i^* + \dot{h}_j^*}{2} \tag{17}$$

for each element the following equation is verified:

$$F_i + F_c + F_p + F_u = 0 \tag{18}$$

which shows how this procedure of evaluation of fluid mass balance preserves the mass.

Since condition (9) of coupling between aquitards and aquifers is comparable to an imposed piezometry condition for aquitards, it would be appropriate to use expression (15) and (16) for the definition of leakage terms L_2 and L_1 indicated in equation (1). These expressions indicate the leakage term as a flow equivalent to the imposed piezometry condition, at top and bottom of the aquitards.

This leakage term expression coincides with that obtained by Fujinawa.[2,3] Applying the Galerkin method to equation (1) we obtain the following linear system:

$$\mathbf{C}\dot{\mathbf{H}} + \mathbf{A}\mathbf{H} = \mathbf{B}$$

$$\mathbf{C} = \begin{bmatrix} \mathbf{C}^0 & \mathbf{C}^{0*} \\ \mathbf{C}^{*0} & \mathbf{C}^* \end{bmatrix}; \quad \mathbf{A} = \begin{bmatrix} \mathbf{A}^0 & \mathbf{A}^{0*} \\ \mathbf{A}^{*0} & \mathbf{A}^* \end{bmatrix}; \quad \mathbf{B} = \begin{bmatrix} \mathbf{b} \\ \mathbf{b}^* \end{bmatrix}; \quad \mathbf{H} = \begin{bmatrix} \mathbf{h} \\ \mathbf{h}^* \end{bmatrix} \tag{19}$$

In this system $\mathbf{C}^0$, $\mathbf{A}^0$, $\mathbf{b}$ and $\mathbf{h}$ represent the discretization of equation (1) on aquifers; and $\mathbf{C}^*$, $\mathbf{A}^*$, $\mathbf{b}^*$ and $\mathbf{h}^*$ the discretization of equations (2) on aquitards. $\mathbf{C}^{0*}$ and $\mathbf{A}^{0*}$ represnt the coupling conditions between aquifers and aquitards and derive from leakage terms L_2 and L_1, whereas $\mathbf{C}^{*0}$ and $\mathbf{A}^{*0}$ represent the coupling conditions between aquitards and aquifers, by assimilating condition (9) of coupling to an imposed piezometry condition on the aquitards. The matrices and right hand term of system (19) are obtained by assembling the matrices and the right hand terms of aquifer and aquitard elements.

For the aquifers, the terms N_i, N_J and N_k are used for linear shape functions of the element associated to the 3 nodes i, j and k. Matrix $\mathbf{A}$ of system (19) is obtained by assembling the following elementary matrices:

$$A_{lm}^1 = \int_{D_e} T\left(\frac{\partial N_l}{\partial x}\frac{\partial N_m}{\partial x} + \frac{\partial N_l}{\partial y}\frac{\partial N_m}{\partial y}\right) dA \tag{20}$$

which contributes to assembly of $\mathbf{A}^0$

$$C_{lm}^5 = \int_{D_e} S N_l N_m\,dA; \qquad l, m = i, j, k \tag{21}$$

which contributes to assembly of $\mathbf{C}^0$. Assuming that the leakage terms on nodes are evaluated on the basis of equations (15) and (16), and that they vary linearly inside the element, we have the following contributions for assembly of matrices $\mathbf{A}$ and $\mathbf{C}$.

$$A_{lm}^3 = \frac{K_m}{\Delta z_m} \int_{D_e} N_l N_m\,dA; \qquad l, m = i, j, k \tag{22}$$

which contributes to the assembly of $\mathbf{A}^0$

$$A_{lm^*}^{*3} = \frac{K_m}{\Delta z_m} \int_{D_e} N_l N_m\,dA; \qquad l, m = i, j, k \qquad m^* = i^*, j^*, k^* \tag{23}$$

The terms i^*, j^*, k^*, indicate the nodes of aquitards in proximity to nodes i, j, and k which are used in (14) and (16). This matrix contributes to the assembly of A^{0*}

$$C^3_{lm} = \frac{S_{sm}\Delta z_m}{3} \int_{D_e} N_l N_m \, dA; \qquad l, m = i, j, k \tag{24}$$

which contributes to the assembly of $\mathbf{C}^0$

$$C^{*3}_{lm^*} = \frac{S_{sm}\Delta z_m}{6} \int_{D_e} N_l N_m \, dA; \qquad l, m = i, j, k \qquad m^* = i^*, j^*, k^* \tag{25}$$

which contributes to the assembly of $\mathbf{C}^{0*}$. In these last 4 formulae K_m indicates the macroelement's permeability of the aquitard related to node m, and S_{sm} indicates the specific storage coefficient related to it. The term Δz instead indicates the thickness of the relative aquitard element.

Finally, formula (12) defines the contributions to the assembly of $\mathbf{A}^*$, $\mathbf{A}^{*0}$, $\mathbf{C}^*$, $\mathbf{C}^{*0}$. The right-hand terms of this system are also obtained by assembling the right-hand terms pertaining to each element. Assuming that the source term used in (1) varies linearly and assumes the values Q_i, Q_j, and Q_k for the 3 elements nodes, we have the following contributions to assembly of the right hand term.

$$b_l = -\sum_m Q_m \int_{D_e} N_l N_m \, dA; \qquad l, m = i, j, k \tag{26}$$

whereas, if $Q = q_0 \delta(x - x_o)\delta(y - y_0)$ represents a concentrated source, with intensity q_0 located at point (x_0, y_0), we have:

$$b_l = -q_0 N_l(x_0, y_0) \tag{27}$$

In particular if point (x_0, y_0) coincides with one of the 3 nodes, for example $l = i$, we have:

$$b_i = -q_0, \qquad b_j = b_k = 0 \tag{28}$$

This observation allows interpretation of the right-hand term of equation (19) related to the aquifer nodes, as for a point source, located at node P_s with an intensity of $-b_s$. Once this has been established, we are able to define the E.N.S. method for fluid mass balance evaluation on aquifers, as described in the following.

Assembly of the right-hand term of system (19) is completed by the contribution which derives from the condition of imposed flow on aquifer:

$$b_l = \int_{\Gamma_e} \varphi_0 N_l \, ds \tag{29}$$

It is obvious that by using the procedure adopted to estimate the leakage terms, the matrices $\mathbf{A}$ and $\mathbf{C}$ of system (19) are symmetric, in relation to the fact that the equations which govern the fluid movement are self-adjoint. This does not occur when using traditional methods, such as those used by Chorley and Frind.[4] The fluid mass balances can be expressed for the aquifers in conservative terms on each element, using a procedure similar to the one used for aquitard elements.

The items used in this fluid mass balance are:

q_1 = distributed source
q_2 = concentrated source
q_3 = top leakage
q_4 = bottom leakage
q_5 = source equivalent to the imposed flow conditions
q_6 = source equivalent to the imposed piezometry conditions
q_7 = fluid deriving from contiguous elements
q_8 = storage depletion

Each of these 8 balance items related to the element can be divided into 3 terms associated with 3 element nodes. The balance terms associated with nodes allow interpretation of the equation of system (19) as balance equations.

As for the balance terms, index e represents the balance terms referred to the element, and indices $m = i, j, k$ represent the same terms referred to element nodes.

q_1 = *distributed sources*

$$q_{1e} = \int_{D_e} Q \, dA; \qquad q_{1m} = \int_{D_e} QN_m \, dA \tag{30}$$

we have $q_{1i} + q_{1j} + q_{1k} = q_{1e}$ since $N_i + N_j + N_k = 1$

q_2 = *concentrated sources*

$$q_{2e} = \sum q_r; \qquad q_{2m} = \sum q_r N_m(x_r, y_r) \tag{31}$$

the sum is applied to all concentrated source terms located on the points (x_r, y_r) inside the element.

q_3, q_4 = *leakage terms.* Using the term L to indicate L_2 or $-L_1$ we have

$$q_{4e}, q_{3e} = \int_{D_e} L \, dA; \qquad q_{4m}, q_{3m} = \int_{D_e} LN_m \, dA \tag{32}$$

Leakage is evaluated on element nodes by using (15) or (16) and interpolating linearly inside the element.

q_5 = *source equivalent to the conditions of imposed flow*

$$q_{5e} = \oint_{\Gamma_e} \varphi \, ds; \qquad q_{5m} = \oint_{\Gamma_e} \varphi N_m \, ds \tag{33}$$

Γ_e is the boundary of element. φ is posed equal to zero for the sides where imposed flow conditions do not exist, and is posed equal to the given flux for the sides where such conditions hold.

q_6 = *source equivalent to conditions of imposed piezometry.* The nodal source equivalent to the imposed piezometry condition on a node, is defined in the same manner for aquifers as for aquitards. It is defined as a point source term, located on a node whose intensity enables to reproduce the same piezometry on the whole system, after having removed the imposed piezometry condition on the node. On the basis of the observations related to formulae (27) and (28), this balance term can be determined starting from the equation obtained by assembling system (19) for the node, as if the conditions of imposed piezometry did not exist.

Using in this equation, the piezometry obtained by the solution of system (19) previously obtained with the imposed piezometry condition, there is a residual, usually not zero, which changed in sign, gives a source term equivalent to the imposed piezometry condition on the node.

$$-q_{6m} = \sum_s a_{ms} h_s + \sum_s c_{ms} \dot{h}_s - b_m \tag{34}$$

The analogous term referred to the imposed piezometry condition on the node, limited to the sole element under observation, is obtained by considering in (34) only the contributions to the equation deriving from assembly of the element

$$-q^e_{6m} = \sum_s a^e_{ms} h_s + \sum_s c^e_{ms} \dot{h}_s - b^e_m$$

where a^e_{ms}, c^e_{ms}, b^e_m indicate the contributions to assembly of the system related to the element.

The source term pertaining by this item to the element, is obtained by adding the contributions q^e_{6m} pertaining to element nodes, subject to imposed piezometry conditions.

q_7 = *fluid deriving from contiguous elements.* In order to define this balance item we will consider the elements which meet on node P_r, divided into 2 parts A and B, as in Figure 5.

Indicating by a^A_{rs}, c^A_{rs}, b^A_r, a^B_{rs}, c^B_{rs}, b^B_r, the contributions to the assembly of equations in system (19) for node P_r, which derive from the two groups of elements meeting on node P_r, we have:

$$\left.\begin{aligned} a_{rs} &= a^A_{rs} + a^B_{rs} \\ c_{rs} &= c^A_{rs} + c^B_{rs} \\ b_r &= b^A_r + b^B_r \end{aligned}\right\} \tag{35}$$

and the equation of system (19) related to node P_r, can be written as:

$$\left.\begin{aligned} \sum a^A_{rs} h_s + \sum c^A_{rs} \dot{h}_s &= b^A_r - q^B_r \\ -q^B_r &= b^B_r - \sum a^B_{rs} h_s - \sum c^B_{rs} \dot{h}_s \end{aligned}\right\} \tag{36}$$

According to the above-said observations, the term q_r can be interpreted as a concentrated source term, located on node P_r. This interpretation allows to define q_r as a source term equivalent to the influence of part B on part A through node P_r. This source term can be

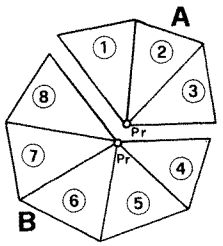

Figure 5. Section of a structure in correspondence to node P_i for evaluation of the nodal source equivalent to the influence of part B on part A through node P_i

evaluated once the system (19) has been solved, and both h_s and $\dot{h}_s$ are known. In this case, to evaluate q_r^B it would be more suitable to use the first of the equations in (36).

$$q_r^B = b_r^A - \sum a_{rs}^A h_s - \sum c_{rs}^A \dot{h}_s \tag{37}$$

The reason for this is that this equation permits evaluation of the fluid flow from part B to part A on node P_r, using the only data deducible from the assembly of the elements found in part A. It should be noted that this balance item, as the preceeding one, similarly to the situation expressed by (15) and (16) for the aquitards, considers also the time derivatives of the piezometry on the nodes. This differs from the traditional estimation methods which consider the spatial gradient. Considering a particular case, the part A under observation is reduced to a single element. Equation (37) becomes:

$$-q_{7m}^e = \sum a_{ms}^e h_s + \sum c_{ms}^e \dot{h}_s - b_m^e \tag{38}$$

and supplies the nodal source term, equivalent to the influence of the remaining structure on the element, through its 3 nodes. Summing these 3 items, one obtains the term q_{7e} pertaining to the element.

$q_8 =$ *storage depletion*

$$q_{8e} = \int_{D_e} S_e \frac{\partial h}{\partial t} \, dA; \qquad q_{8m} = \int_{D_e} S_e \frac{\partial h}{\partial t} N_m \, dA \tag{39}$$

It is easy to ascertain that this procedure for evaluation of fluid mass balance on the element, is conservative. In fact, by summing the 3 expressions which supply the fluid deriving from contiguous elements on 3 elements nodes:

$$\left.\begin{aligned} q_i^B &= b_i^e - \sum a_{is}^e h_s - \sum c_{is}^e \dot{h}_s \\ q_j^B &= b_j^e - \sum a_{js}^e h_s - \sum c_{js}^e \dot{h}_s \\ q_k^B &= b_k^e - \sum a_{ks}^e h_s - \sum c_{ks}^e \dot{h}_s \end{aligned}\right\} \tag{40}$$

we obtain the following equation:

$$q_{1e} + q_{2e} + \ldots + q_{8e} = 0 \tag{41}$$

Moreover, the equations of system (19) on this basis can be rigorously interpreted as balance equations, regarding the equivalent nodal sources which act upon each node. This procedure permits the evaluation of fluid mass flow, through any aquifer section, as the sum of the nodal sources, equivalent to the action of part B on part A, for all the nodes of the section line. Figure 6 illustrates this situation. This balance evaluation along the line is conservative, in the sense that it could be made both on the basis of data related to part A and those related to part B, and both values coincide.

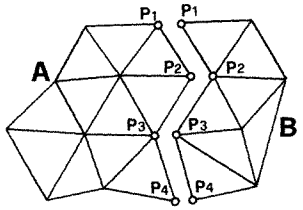

Figure 6. Section of a structure along a line for the evaluation on the flow of fluid mass, as the sum of nodal sources equivalent on the line nodes

By evaluating the fluid mass flow through the branching lines in this manner, condition (6) of mass conservation along the branching line is rigorously verified.

The above-mentioned method for balance evaluation is applicable also to analogous equations which govern other physical phenomena such as distribution of electrical or thermal fields, and can be extended to the three-dimensional case. It could be formulated also in the case of a general shape function.

NUMERICAL SOLUTION IN STEADY STATE CASE

In the steady state case, the discretization of finite element brings to a system of ordinary linear equations.

$$\mathbf{Ah} = \mathbf{b} \tag{42}$$

With a uniform permeability along the z-axis, the piezometry trend along this axis is linear and every aquitard macroelement can be reduced to a single element.

The matrix $\mathbf{A}$, in this case is limited to part $\mathbf{A}^0$. The steady state equations are used only for calibration of the mathematical model, consisting in the solution by various attempts of an inverse problem. In this case the piezometry is known in advance and thus the wet thickness in the acquifer's phreatic zones.

For this reason, it is possible to use equations of aquifers under pressure even in phreatic zones, and system (42) thus results linear. Particularly suitable is the frontal method of Irons[5] for the solution of similar systems, especially if applied to two-dimensional cases. This method is substantially a method of Gaussian type elimination, without pivot, which combines the forward elimination of variables, with that of system matrix assembly. Order of elimination of variables is guided by the order of element assembly. One variable is eliminated as soon as the assembly of all elements which refer to it is complete. All the variables which appear during the assembly of elements (since one or more elements refer to them), and are not yet eliminated (because other elements not yet assembled refer to them) form the active variables front.

The active variables front varies dynamically during the forward elimination and the back substitution. Application of the frontal method in our case, similarly to three-dimensional cases, sets the same limits to the problems which can be treated, owing to the high number of active variables which we can have in the front. In our case this is due to 2 causes: aquifer branching and presence of aquitards. The method which we propose eliminates this problem.

The front increase caused by aquifer branching is limited when resorting to the substructuring. This permits a temporary elimination, from the active variables front, of the variables corresponding to the branching lines. These appear subsequently, when only the variables of bordering nodes between substructures are processed. Introduction of substructuring into the frontal method develops as follows.

In every substructure the bordering nodes between substructures are indicated by using a negative number. All the negative nodes of a substructure define the pseudoelement of the structure. The substructures are examined one by one for assembly and forward elimination. During this stage the variables with negative number are never eliminated.

By processing all the elements of a substructure, the residual active variables front defines the pseudo-element of the substructure which is registered on appropriate file. The residual matrix in memory related to the contributions of the variables already eliminated in the substructure to element assembly and forward elimination, and the same right hand term, form the stiffness matrix and right-hand term of the pseudo-element. They are registered in appropriate files to be processed subsequently.

After having processed the substructures in this manner, all the variables with positive numbers are subjected to a forward elimination process.

At this point the substructure pseudoelements are processed as normal elements within the fontal method, thus concluding the forward elimination phase for variables with negative numbers. The back substitution concerns at first the pseudoelements, for which we obtain an output for elements registered in the appropriate file. Thus, one proceeds to the phase of back substitution in the single substructures. The substructures are examined inversely. The memory zone which should contain the piezometry in the back substitution processes of the frontal method is initialized with the piezometry of the respective pseudoelement taken from the appropriate file. Subsequently the substructure elements are processed for back substitution. This method is used for all substructures. For the efficiency of this method, the branching line nodes should coincide with the bordering nodes between substructures.

However, the substructuring technique does not solve the problem of front increase caused by the presence of aquitards, which relate the nodes of one level to those of the underlying level. The variables of nodes subject to leakage remain in the active variables front, until all the elements which refer to it in every level, have been assembled. In order to solve this other problem, we inserted an iterative process within the substructured frontal method. The above process transfers the contribution of the leakage, to the right-hand side of the equations. This iterative method employs a forcing technique of iterations. The optimal forcing factor is automatically evaluated by using a few iterations without forcing. During calibration of the mathematical model, numerous calculations are carried out on the same network. Each of these calculations differs from the previous one in a few variations made to the boundary conditions or to the physical parameters.

Usually, these variations only slightly affect the computed forcing factor of iterations. In the major part of these cases it is possible to exclude automatic calculation of the forcing factor by using the value determined in a previous elaboration, thus avoiding the related iteration process. Following is a description of the simple iteration method used to estimate the forcing factor, of the forced iteration method and of the iterated frontal method. The latter represents the implementation of the forced iteration method with automatic calculation of the forcing factor, within the substructured frontal method, and is the numerical method used to solve system (42). The formulation of these iterative methods considers matrix $\mathbf{A}$ of system (42) split into 2 addends:

$$\mathbf{A} = \mathbf{A}_0 + \mathbf{A}_1 \tag{43}$$

where part $\mathbf{A}_1$ derives from the assembly of contributions due to leakage, expressed by formulae (22) and (23). System (42) can now be written as follows:

$$\mathbf{A}_0\mathbf{h} = \mathbf{b} - \mathbf{A}_1\mathbf{h} \tag{44}$$

From the system written as above we can deduce 2 iterative processes.

(a) *Simple iteration method*

This is obtained by iteratively applying the following relation:

$$\mathbf{A}_0\mathbf{h}^n = \mathbf{b} - \mathbf{A}_1\mathbf{h}^{n-1} \tag{45}$$

with $\mathbf{h}^0 = \mathbf{0}$.

This iterative scheme determines firstly solution $\mathbf{h}^1$ assuming that the aquitards are impermeable. Subsequently, on the basis of this piezometry, the leakage terms are determined using (15) and (16) (without time terms in this case) and transferring everything to the right hand term.

Thus, a new piezometry is determined iteratively. Indicated as:

$$\boldsymbol{\varepsilon}^n = \mathbf{h}^n - \mathbf{h} \tag{46}$$

the difference between the nth iteration and the solution of system (42), this error will propagate with the following law:

$$\boldsymbol{\varepsilon}^n = \mathbf{P}\boldsymbol{\varepsilon}^{n-1} \tag{47}$$

$$\mathbf{P} = -\mathbf{A}_0^{-1}\mathbf{A}_1 \tag{48}$$

the iterative process (45) is convergent if and only if all the eigenvalues of $\mathbf{P}$ have modulus less than one. Relations (22) and (23) define those matrices that, when assembled, produce $\mathbf{A}_1$. These relations point out that the $\mathbf{A}_1$ matrix terms (and thus the $\mathbf{P}$ matrix terms) are directly proportional to aquitard permeability and inversely proportional to the thickness.

Consequently, even the dominating eigenvalue of the matrix $\mathbf{P}$ is directly proportional to the permeability and inversely proportional to the aquitard thickness. Therefore, we can see that the above-mentioned process does not always converge. In particular, it does not converge for problems with high permeability aquitards and small thickness. Moreover, when the iterative method is convergent, convergence is faster for higher thickness and lower permeability in aquitards. Another important aspect for the following considerations is that the described iterative procedure, both when it converges and when it diverges, presents a fluctuating behaviour.

This fact was experimented by us in all its numerous applications to practical cases and hypothetical ones.

(b) *Method of forced interations*

The system described as in (44) brings to the second iterative scheme:

$$\mathbf{A}_0(\mathbf{h}^n - \mathbf{h}^{n-1}) = \alpha(\mathbf{b} - \mathbf{A}\mathbf{h}^{n-1}) \tag{49}$$

where α indicates the forcing factor of iterations. The iterative scheme can be written as follows:

$$\mathbf{h}^n = (1-\alpha)\mathbf{I}\mathbf{h}^{n-1} + \alpha\mathbf{A}_0^{-1}(\mathbf{b} - \mathbf{A}_1\mathbf{h}^{n-1}) \tag{50}$$

To study the convergence of this second iterative scheme we analyse the eigenvalues of matrix $\bar{\mathbf{P}}$ which guides the propagation of error;

$$\bar{\mathbf{P}} = (1-\alpha)\mathbf{I} + \alpha\mathbf{P} \tag{51}$$

Since this matrix is expressed by a linear polynomial in matrix $\mathbf{P}$, which in turn expressed the propagation of error in the previous iterative scheme, we can deduce that the eigenvalues of the two matrices are tied by the same linear relation:

$$\mu = (1-\alpha) + \alpha\lambda \tag{52}$$

μ indicates the eigenvalues of $\bar{\mathbf{P}}$ and λ those of $\mathbf{P}$. This equation is represented graphically by a bundle of straight lines having centre at the point (1, 1) of the (λ, μ) plane as illustrated in Figure 7.

The oscillating trend of the iterative solution technique (45) points out that the dominating eigenvalue of matrix $\mathbf{P}$ is real ($\mathbf{P}$ is symmetrical) and negative. The eigenvalues of $\mathbf{P}$ can be ordered as follows:

$$\lambda_0 \leqslant \lambda_1 \leqslant \ldots \leqslant \lambda_n \tag{53}$$

where λ_0 is the dominating eigenvalue.

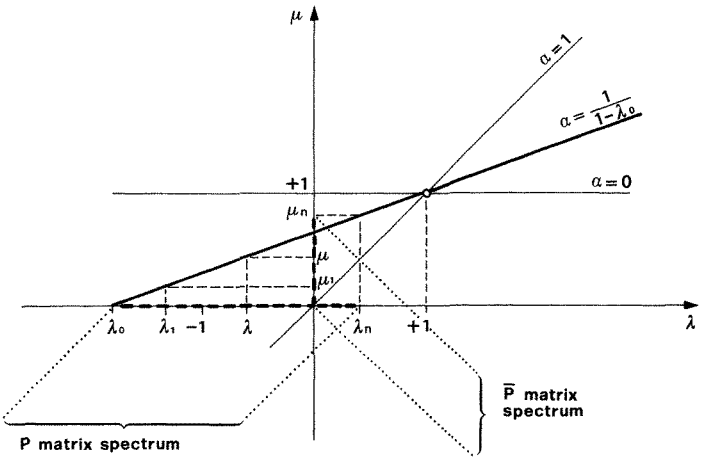

Figure 7. Relationship between eigenvalues of **P** and $\bar{\mathbf{P}}$

We will consider in this iterative solution technique, that particular forcing factor α_0 which in equation (52) changes the dominating eigenvalue of **P** to 0.

$$\alpha_0 = \frac{1}{1-\lambda_0} \tag{54}$$

As can be observed in Figure 7, in this case all the negative eigenvalues of matrix **P** are transformed into positive and less than 1 eigenvalues (in fact less than $1-\alpha_0$).

Eventual positive eigenvalues less than 1 of **P** remain positive and less than 1 in $\bar{\mathbf{P}}$. Thus we can assume that this second iterative scheme is convergent even when the first scheme is not convergent, provided that the dominating eigenvalues of **P** is negative and **P** does not include positive eigenvalues higher than 1 in its spectrum.

(c) *The iterated frontal method*

The frontal method is a Gaussian method and thus for the solution of system (42) uses a factorization of matrix **A** in the form of:

where:
$$\mathbf{A} = \mathbf{L}\mathbf{D}\mathbf{L}^T \tag{55}$$

D = diagonal matrix
L = lower triangular matrix

In the forward elimination phase the system is written in the equivalent form:

$$\mathbf{U}\mathbf{h} = \mathbf{b}^* \tag{56}$$

with

$$\mathbf{U} = \mathbf{D}\mathbf{L}^T \tag{57}$$

$$\mathbf{b}^* = \mathbf{L}^{-1}\mathbf{b} \tag{58}$$

In the back substitution phase the system is solved and the following solution is obtained:

$$\mathbf{h} = \mathbf{U}^{-1}\mathbf{b}^* \tag{59}$$

Eventual subsequent solutions of the same system with different right-hand terms can be obtained in 'resolution', by using the previously calculated matrix **U**.

This operation is possible because the matrix $\mathbf{L}^{-1}$, necessary to determine the right hand term of system (59) in relation to the new case, can be expressed by using the factorization of $(n-1)$ elementary matrices:

$$\mathbf{L}^{-1} = \mathbf{L}^{(n-1)}\mathbf{L}^{(n-2)} \ldots \mathbf{L}^{(1)} \tag{60}$$

Each of these matrices is lower triangular with all the terms of the diagonal equal to 1, and all the extradiagonal terms equal to zero, except those of column s for matrix $\mathbf{L}^{(s)}$. These terms are obtained by using the corresponding terms of the s row of $\mathbf{U}$ by means of the simple relation:

$$l_{is} = \frac{u_{is}}{u_{ss}} \tag{61}$$

The iterative method used with the frontal method is substantially the forced iteration method as described previously. However, a few initial iterations are carried out with the first iterative method so as to estimate the dominating eigenvalue of the matrix $\mathbf{P}$ and thus define the forcing factor in the second iterative method. Three iterations results to be suitable for this objective, in all the practical applications made by us.

Indicating the mean quadratic residual as:

$$\sigma_n = \|\mathbf{h}^{(n)} - \mathbf{h}^{(n-1)}\| \tag{62}$$

the following

$$\xi_n = \frac{\sigma_n}{\sigma_{n-1}} \tag{63}$$

represents an estimate of the dominating eigenvalue of matrix $\mathbf{P}$. In order to define λ_0 we will consider the average of the last 2 values of ξ

$$s_0 = \tfrac{1}{2}(\xi_2 + \xi_3) \tag{64}$$

and considering

$$\lambda_0 = -s_0 \tag{65}$$

In this case, the dominating eigenvalue of $\mathbf{P}$ is negative. The estimate of α_0 is given by

$$\alpha_0 = \frac{1}{1+s_0} \tag{66}$$

In the iterated frontal method the first iteration is determined by considering the leakage terms as null. The three following simple iterations are made in resolution. By using the piezometry of the last iteration carried out, the system's right-hand term is updated with the leakage terms expressed in formulae (15) and (16). By applying the resolution procedure to the obtained right-hand term, the result is:

$$\mathbf{b}^{**(n)} = \mathbf{L}^{-1}(\mathbf{b} - \mathbf{A}_1\mathbf{h}^{(n-1)}) \tag{67}$$

and one proceeds with a back substitution in equation (59):

$$\mathbf{b}^{*(n)} = \mathbf{b}^{**(n)} \tag{68}$$

We then proceed to forcing iterations. For this purpose, on the basis of equation (66) the forcing factor is defined.

We start from the last previous iteration if the dominating eigenvalue of $\mathbf{P}$ is estimated to have modulus less than one. In the opposite case, we should start from the initial iteration. In this case the right-hand term is updated on the basis of the leakage terms expressed by (15)

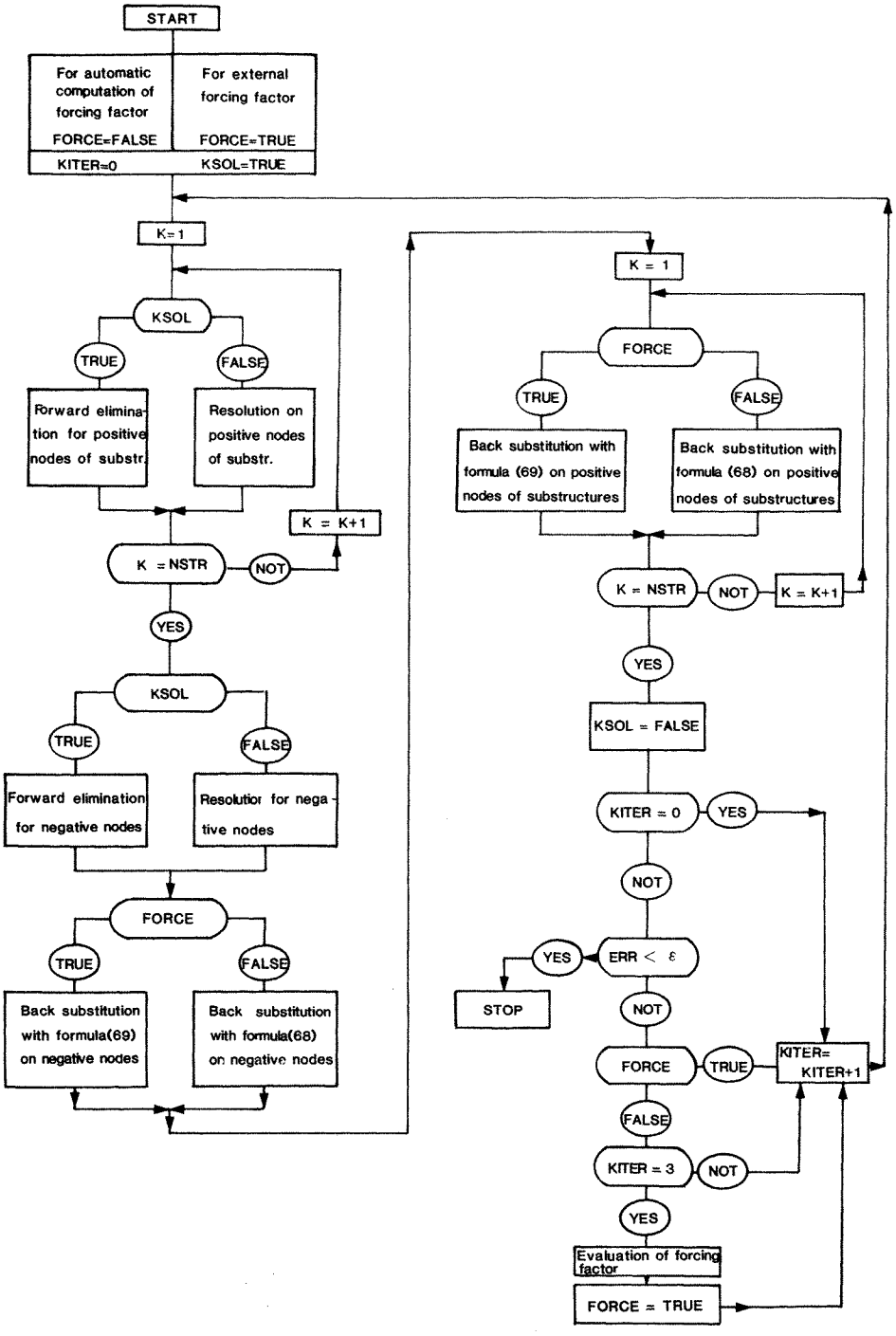

Figure 8. Flow chart of the iterated frontal method

and (16) with the last available piezometry. The right-hand term is processed in resolution according to equation (67). In the back substitution phase this method differs from the first by applying in equation (59) the following right-hand term:

$$\mathbf{b}^{*(n)} = (1-\alpha_0)\mathbf{b}^{*(n-1)} + \alpha_0 \mathbf{b}^{**(n)} \tag{69}$$

The resolution routine with the substructured frontal method uses a couple of files each for all the variables interested by the iterative processes (piezometry and right-hand terms). The first file, containing the variables related to the proceeding iteration, operates in reading. The second, related to the present iteration, operates in writing. On conclusion of each iteration the role of the two files is exchanged.

Figure 8 illustrates the flowchart of the iterated frontal method. In this figure FORCE represents a logical variable which assumes the value TRUE corresponding to the forced iterations, and FALSE for the simple ones. KITER is the iterations counter. KSOL is the logical variable which is TRUE in solution and FALSE in resolution. NSTR is the number of considered substructures. ERR is the mean quadratic residual between the two iterations and ε is the tolerance.

NUMERICAL SOLUTION FOR THE UNSTEADY CASE

The numerical solution for the unsteady case is given by a predictor–corrector procedure. Use of the Crank–Nicolson method for the solution of the differential equations of system (19) deriving from the finite element discretization, points out the same problems for the solution of the frontal method as in the steady case.

The problem is more complicated, owing to the non-linearity of the system in relation to the phreatic zone and to the dependence of the right-hand term on the piezometry. This last factor occurs in relation to particular requirements of the hydrogeological models, especially in relation to problems of aquifer–river exchange.

The proposed method solves these problems retaining the performance of the Crank–Nicolson method. The differential equation system (19) could be written in an equivalent form:

$$\mathbf{C}_0\dot{\mathbf{h}} + \mathbf{A}_0\mathbf{h} = \mathbf{b} - \mathbf{C}^{0*}\dot{\mathbf{h}}^* - \mathbf{C}_1\dot{\mathbf{h}} - \mathbf{A}^{0*}\mathbf{h}^* - \mathbf{A}_1\mathbf{h} \tag{70}$$

$$\mathbf{C}^*\dot{\mathbf{h}}^* + \mathbf{A}^*\mathbf{h}^* = \mathbf{b}^* - \mathbf{C}^{*0}\dot{\mathbf{h}} - \mathbf{A}^{*0}\mathbf{h} \tag{71}$$

with

$$\mathbf{C}^0 = \mathbf{C}_0 + \mathbf{C}_1 \tag{72}$$

$$\mathbf{A}^0 = \mathbf{A}_0 + \mathbf{A}_1 \tag{73}$$

$\mathbf{C}_0$ and $\mathbf{A}_0$ are obtained from $\mathbf{C}^0$ and $\mathbf{A}^0$ without considering the contribution to their assembly, due to leakage, given by equations (24), (25), (22) and (23) respectively.

The leakage contributions define the matrices $\mathbf{C}_1$ and $\mathbf{A}_1$. The predictor–corrector procedure initially determines the predictor piezometry for all the aquifer nodes subject to leakage.

This piezometry defines the right-hand term of system (71) thus resolving it by resorting to the Crank–Nicolson methods, and Thomas method for the linear system (since the relative matrix is tridiagonal).

In this way the predictor piezometry on the aquitards is obtained, and thus the predictor estimate of leakage is calculated. These appear on the right of system (70). It thus determines the corrector piezometry on the aquifers, discretizing initially the time part with the Crank–Nicolson method, and solving the resulting linear system with the substructured

frontal method previously described. The timestep calculation is concluded by the determination of the corrector piezometry on aquitards, which is determined using the same procedure as for the predictor piezometry on aquitards. The only difference is that the right-hand term of equation (71) is determined on the basis of the corrector piezometry on aquifers. The time advancement scheme of the predictor–corrector method is based on a sequence of time macrosteps. Each time macrostep is composed of an arbitrary number of timestep; all of the same length. This permits one to have the forward elimination phase with the frontal method only at the beginning of each macrostep, operating in resolution for all the subsequent steps of the macrostep, thus saving a lot of C.P.U. time. At the beginning of each macrostep, the matrix of the system in phreatic zones is updated.

Time dependence of the source terms and boundary conditions is represented by associating to them time functions of the step or straight segments type. In the same manner, we should take into account the dependence of punctual source terms on the piezometry.

Figure 9 reproduces the flow chart of the temporal iteration. In it, KSTEP is the counter of the timesteps inside a macrostep composed of NSTEP steps. The substructured frontal method operates in solution when KSTEP = 0 (at the beginning of the macrostep), and in resolution when KSTEP $\neq 0$. No iteration is operated since the leakage evaluated by means of predictor piezometrics appears on the equation's right-hand term.

Predictor piezometry on aquifers

The predictor piezometry on aquifers is determined for each node subject to leakage, solving the system of differential equations (74) with an explicit procedure:

$$\mathbf{C}_{0l}\dot{\mathbf{h}} + \mathbf{A}_0\mathbf{h} = \mathbf{b} - \mathbf{C}^{0*}\dot{\mathbf{h}}^* - \mathbf{C}_1\dot{\mathbf{h}} - \mathbf{A}^{0*}\mathbf{h}^* - \mathbf{A}_1\mathbf{h} \tag{74}$$

This system is analogous to system (70) and is obtained by evaluating matrix $\mathbf{C}_0$ using a lumped capacity, that is by assuming that the storage coefficient S to be used in (21), is concentrated on the 3 nodes of each element, instead of being distributed on the element. As a result, equation (21) becomes:

$$C^5_{l,m} = \frac{SD_e}{3}\delta_{l,m} \tag{75}$$

where D_e is the element area and $\delta_{l,m}$ is the Kroneker symbol. Thus matrix $\mathbf{C}_{0l}$ is diagonal.

To estimate the right-hand term of system (74) the piezometry of the time t^n is considered. System (74) with the explicit procedure of time discretization becomes:

$$\frac{1}{\Delta t}\mathbf{C}_{0l}(\mathbf{h}^{n+1} - \mathbf{h}^n) + \mathbf{A}_0\mathbf{h}^n = \mathbf{b}^n \tag{76}$$

where $\mathbf{b}^n$ is the right-hand term of system (74) evaluated with the piezometry of the time t^n. This system, owing to the fact that matrix $\mathbf{C}_0$ is diagonal, permits the solution of the system, obtaining $\mathbf{h}^{n+1}$ on each node subject to leakage.

In two different circumstances this procedure is not adequate and causes a high fluctuation of the solution. The first case occurs in the case of nodes near which considerable water extractions exist, with high values of the time increment Δt. The cause of this is that the term $\mathbf{A}h^n$, which in (76) represents the flow of fluid on the node, deriving from contiguous nodes, is evaluated on the basis of the piezometry of the time t^n. Consequently, this evaluation does not take into account the evolution of piezometry on the time interval Δt.

To overcome the above difficulty we have introduced an alternative method for evaluation of predictor piezometry for all nodes which, based on the previous evaluations, present a piezometric variation exceeding 10 m. Using this method, to determine the drawdown on

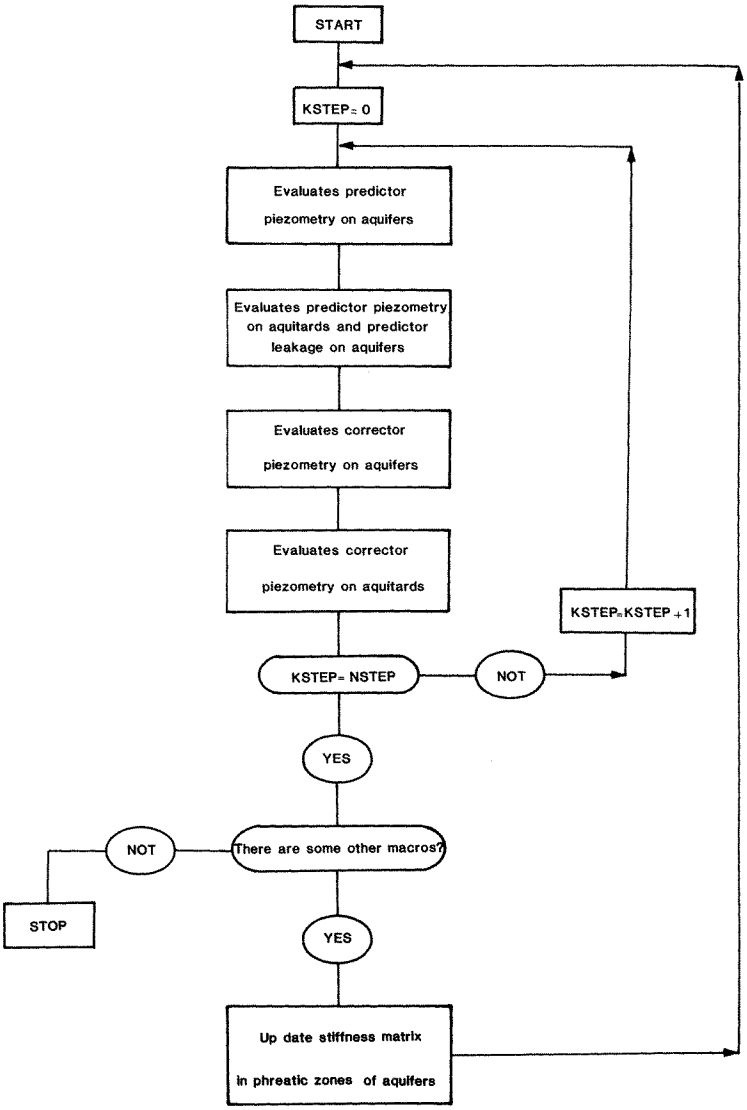

Figure 9. Flow chart of the time iterations

node P_i, we will imagine that all source terms acting on the elements converging into node P_i are located on the element's barycentre, and assimilated to punctual source terms. The equivalent punctual source Q_k term represent all the sources in the element. The distributed ones, which if depending on time, are evaluated at $t+\Delta t$, and the leakage evaluated on the basis of piezometry at time t.

Drawdown on node P_i is estimated as the sum of the drawdown pertaining to each source term located on the element barycentres, defined on the basis of the Theis formula:

$$\Delta h_i = \sum \Delta h_{ik} \tag{77}$$

$$\Delta h_{ik} = \frac{Q_k}{4\pi T_k} \mathrm{Ei}\left(-\frac{1}{4}\frac{S_k}{T_k}\frac{R_k^2}{\Delta t}\right) \tag{78}$$

where:

Q_k = punctual source term equivalent to source terms and leakage operating on the element
S_k = storage coefficient on the element k
T_k = transmissivity on the element k
R_k = distince of node P_i from barycentre of element k
Δt = time increment
Ei(x) represents the Exponential Integral function

The second case in which the explicit method becomes critical is represented by the case of source points with piezometric control. For this case, a predictor procedure is adopted which purposely takes into account the law of dependence of punctual source terms to piezometry. We will use q to indicate the source term value as a piezometry function:

$$q = q^* f(h(P)) \tag{79}$$

q^* is the constant reference source term and $f(h)$ is the law of dependence on the piezometry on point P.

By using the explicit procedure for time discretization as in equation (76), with the lumped capacity method to define the matrix $\mathbf{C}_{0l}$, we can express the increase Δh_m of piezometry on 3 nodes i, j, k, of the element in function of the equation's right-hand term:

$$\Delta h_m = \frac{\Delta t}{\left(\frac{\sum_e S_e D_e}{3}\right)_m} \left(b_m - \sum_s a_{ms} h_s\right) \tag{80}$$

$m = i, j, k$
S_e = storage coefficient of the e-element converging on the node m
D_e = area of element e

The denominator sum is extended to all elements converging on node m. We will divide the right-hand term b_m which appears in this formula, in two parts:

$$b_m = b'_m + b''_m \tag{81}$$

the part b''_m is the part depending on the piezometry due to the presence in the element of the piezometric-controlled source term, whereas b'_m is the part not dependent on it. For equations (27) and (29) we have:

$$b''_m = -q^* n_{m^0} f(h_0) \tag{82}$$

with

$$n_{m^0} = N_m(x_0, y_0)$$

where N_m is the shape function pertaining to node m and h_0 is the piezometry on point P at time $t + \Delta t$ which can be expressed according to the 3 node piezometry at time $t + \Delta t$.

$$h_0 = \sum_m n_{m0}(h_m + \Delta h_m), \qquad m = i, j, k \tag{83}$$

where h_m is the piezometry at time t on node m. For equations (80) and (82) we have :

$$h_m = A_m - \bar{n}_{m0} f(h_0) \tag{84}$$

$$A_m = \frac{\Delta t}{\left(\frac{\sum S_e D_e}{3}\right)_m} \left(b_m - \sum a_{ms} h_s\right) \tag{85}$$

$$\bar{n}_{m0} = \frac{\Delta t}{\left(\frac{\sum S_e D_e}{3}\right)_m} q^* n_{m0} \tag{86}$$

By applying these functions in equation (83) we obtain the following:

$$h_0 = K - Mf(h_0) \tag{87}$$

$$K = \sum_m n_{m0}(h_m + A_m); \qquad m = i, j, k \tag{88}$$

$$M = \sum_m n_{m0} \bar{n}_{m0}; \qquad m = i, j, k \tag{89}$$

Assuming that function $f(h)$ in equation (79) is the straight line:

$$f(h) = \alpha + \beta h \tag{90}$$

The equation (87) admists only a single root given by:

$$h_0 = \frac{K - \alpha M}{1 + \beta M} \tag{91}$$

In the general case, where $f(h)$ is represented by a step or straight segment function defined by points:

$$(h_1, f_1) \cdots (h_N, f_N) \tag{92}$$

several or no roots of equation (87) may exist. For this case, assuming h_{00} as the piezometry on point P at time t, we can point out the interval of definition of the function as:

$$h_r \leqslant h_{00} \leqslant h_{r+1}$$

(eventually $h_r = -\infty$, $h_{r+1} = +\infty$). We consider therefore the root given by formula (91) with coefficients related to the straight line which represents the function in that interval. If the obtained root still belongs to this interval, it is considered as the piezometry on the point at time $t + \Delta t$. In the opposite case, all the intervals are examined and if there are several roots, the one closest to h_{00} is chosen. In the event of total lock of roots in equation (79) h_{00} is assumed as the value of predictor piezometry.

Corrector piezometry on the aquifers

The corrector piezometry is determined by applying the Crank–Nicolson method to system (70), where the right-hand term is evaluated by using the predictor piezometry. Thus the following scheme results:

$$\frac{1}{\Delta t} \mathbf{C}_0(\mathbf{h}^{n+1} - \mathbf{h}^n) + \tfrac{1}{2}\mathbf{A}_0(\mathbf{h}^{n+1} + \mathbf{h}^n) = \tfrac{1}{2}(\mathbf{b}^{n+1} + \mathbf{b}^n), \qquad \Delta t = t^{n+1} - t^n \tag{93}$$

which gives rise to the following linear system:

$$\mathbf{A}\mathbf{h}^{n+1} = \tilde{\mathbf{A}}\mathbf{h}^{n} + \tilde{\mathbf{b}}^{n+1} \tag{94}$$

$$\mathbf{A} = \tfrac{1}{2}\mathbf{A}_0 + \frac{1}{\Delta t}\mathbf{C}_0 \tag{95}$$

$$\tilde{\mathbf{A}} = -\tfrac{1}{2}\mathbf{A}_0 + \frac{1}{\Delta t}\mathbf{C}_0 \tag{96}$$

$$\tilde{\mathbf{b}}^{n+1} = \tfrac{1}{2}(\mathbf{b}^{n+1} + \mathbf{b}^{n}) \tag{97}$$

System (94) is solved by using the substructured frontal method. The solution occurs with assembly of equations and forward eliminations at the beginning of each macrostep, and in resolution for every other step of the time macrostep.

Predictor and corrector piezometry on aquitards

The predictor and corrector piezometry is determined with the same procedure on each aquitard macroelement. Application of the Crank–Nicolson method to the equation of system (71) related to internal nodes of each aquitard macroelement, yields a system analogous to system (94), in which the system matrix is tridiagonal. Therefore to solve this system, the Thomas method is applied.

Timestep selection

Selection of the timestep is conditioned by the stability of the Crank–Nicolson method. As demonstrated by Smith,[6] this method is characterized by a critical timestep, above which the numerical solution oscillates around the theoretical one. This critical timestep depends on the maximum eigenvalue of matrix $\mathbf{C}^{-1}\mathbf{A}$ ($\mathbf{C}$ and $\mathbf{A}$ matrices of system (19)) and cannot be estimated beforehand. Any fluctuations in the calculation indicate however that this critical timestep has been surpassed and thus the elaboration step must be reduced. A step equal to half of the critical one is suitable for most of the applications. A smaller step uselessly takes up C.P.U. time without improving the obtained solution. The first calibration elaborations in the unsteady state are used to point out the critical step through various attempts.

This numerical method differs from the conventional Crank–Nicolson one, by introducing the predictor estimate which allows one to decouple the aquifer equations from those of the aquitards in the corrector phase. The difference between the predictor and the corrector piezometry provides a measure of the inaccuracy introduced in this manner. An appropriate precision indicator is elaborated to check this inaccuracy. It is given by the quotient between the sum of absolute values of the differences between predictor and corrector piezometries at time $t+\Delta t$ and sum of the absolute value of the corrector piezometry increase, between time t and $t+\Delta t$. This sum is extended to all the nodes subject to evaluation of the predictor piezometry. When this indicator assumes values near to or greater than 1, the timestep must be reduced. This indicator is also efficient to indicate the approach or exceeding of the critical timestep of the Crank–Nicolson method.

In practical cases, this indicator has demonstrated that the approximation introduced by the predictor estimate and by the decoupling between aquifers and aquitards is not worthy of mention for steps equal or less than one half of the critical one.

Comparison with iterative methods

The illustrated method is more suitable for these applications than the conventional iterative methods, and in particular it should be preferred to S.O.R. In these iterative methods, the number of iterations required for the solution of each step depends both on the maximum eigenvalue of the error propagation matrix, and on the distance between the solution to time $t+\Delta t$ and the solution to time t, which defines the timestep's initial iteration.

For this problem, the longer the timestep is, the more iterations are necessary to obtain the solution. Furthermore, considerable piezometric variations occur in relation to abrupt source term variations; the piezometric variations require a major number of iterations to reach the solution. This fact is very frequent in the simulation of real aquifer systems in relation to the exploitation history of aquifer bodies and to the hypothesis to be simulated.

With the conventional iterative methods, if there is a rapid source term variation, it often becomes necessary to adopt a time progression scheme in geometric progression with timesteps which are considerably smaller than one half of the Crank–Nicolson critical step. This serves to reduce the total number of iterations required for the solution. Since the substructured frontal method is a direct solution method, it is not influenced by these factors in relation to the elaboration time and permits the use of the maximum timestep allowed by the Crank–Nicolson method.

The fundamental arithmetical operations carried out in resolution regime for the timestep solution are the same requested to carry out two matrix products per vector with a bandwidth equal to the front's average value. This can be inferred from (60) and (61).

APPLICATIONS

The illustrated method was verified in a hypothetical case of an interconnected aquifer systems, reproduced in Figure 10. Thus it was possible to determine its analytical solution in a steady state case. The boundary conditions, the physical parameters and the source terms

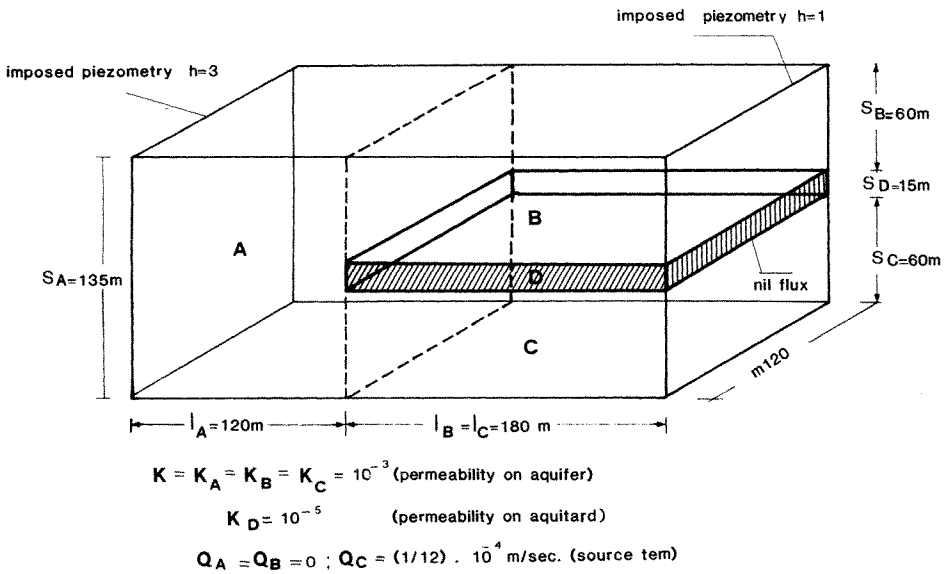

Figure 10. Hypothetical interconnected aquifer system with two aquifer levels, a branching line and an aquitard

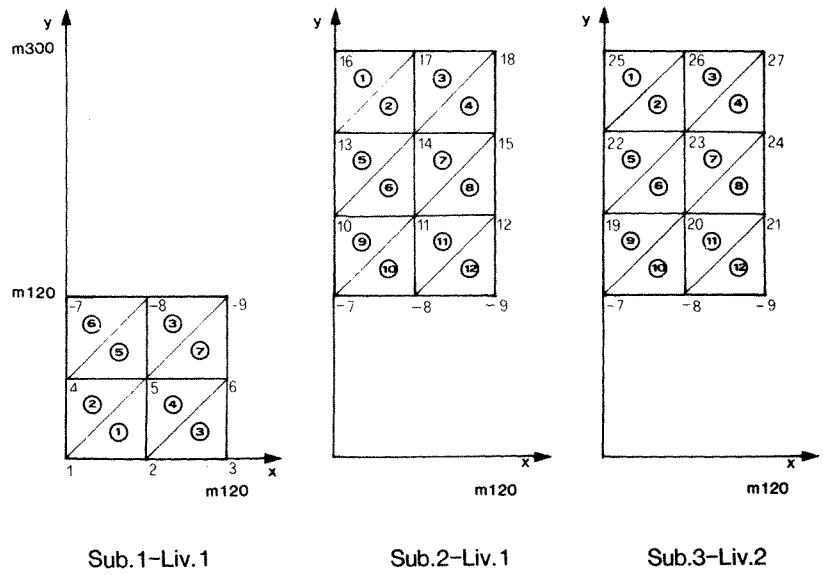

Figure 11. Schematization of finite elements, with three substructures of the interconnected aquifer system of Figure 10. Coarse network (32 aquifer elements, 9 aquitard elements, 27 nodes)

were assigned in a uniform manner in order to obtain a one-dimensional case. The corresponding theoretical solution is given by the following equation:

$$\left.\begin{aligned} h_A &= C_5 y + 3, && 0 \leq y \leq 120 \\ h_B &= C_1 e^{y\sqrt{(2a)}} + C_2 e^{-y\sqrt{(2a)}} + C_3 y + C_4 + y^2 \frac{b}{4}, && 120 \leq y \leq 300 \\ h_C &= -C_1 e^{y\sqrt{(2a)}} - C_2 e^{-y\sqrt{(2a)}} + C_3 y + \left(\frac{y^2 b}{4} - \frac{b}{2a}\right) + C_4, && 120 \leq y \leq 300 \end{aligned}\right\} \quad (98)$$

where:

$$a = \frac{K_D}{s_D}\frac{1}{sK} = 1{\cdot}1111111 \times 10^{-5} \quad (s = s_B = s_C)$$

$$b = \frac{Q_C}{sK} = 1{\cdot}3888888 \times 10^{-4}$$

$C_1 = -0{\cdot}31566949$
$C_2 = -4{\cdot}5234994$
$C_3 = -0{\cdot}021769963$
$C_4 = \ 6{\cdot}8041551$
$C_5 = -0{\cdot}011943671$

Figure 11 illustrates the schematization of the finite elements adopted. The aquifers have been divided by means of 3 substructures with reference to the subdivision in 3 water bodies, as illustrated in Figure 10. Figure 12 reproduces the comparison between the analytical solution and the finite element calculation along the middle section.

Figure 13 illustrates the fluid mass balance on the system's 3 aquifers and the reciprocal fluid's mass exchanges, calculated analytically starting from (98) applying the Darcy law.

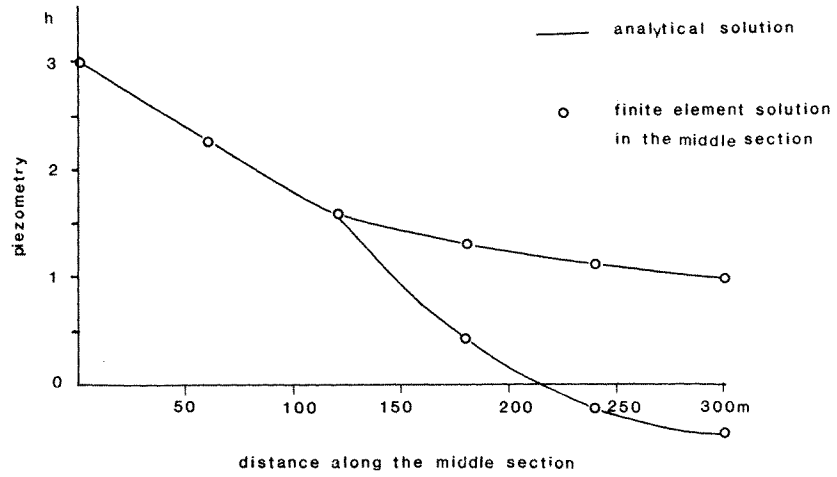

Figure 12. Comparison between theoretical solution and finite element solution along the middle section for the cases of Figure 10 and Figure 11

In Table I the balance evaluated with the E.N.S. method is indicated alongside the analytical balance. The same balance, evaluated with the conventional method starting from the finite element solution, is illustrated. The conventional evaluation is obtained by estimating the piezometry gradient in the y-axis direction, on the basis of the linear shape function. A constant gradient value is assumed along the $y = 0$, $y = 120$ and $y = 300$ line, an average of the three values on the three line's nodes. Using this gradient and applying the Darcy law, it is possible to obtain the source term equivalent to the imposed piezometry conditions and the flow outgoing from the branching lines indicated in Table I.

According to Table I it results that the two methods give practically the same value for source terms equivalent to imposed piezometry conditions for $y = 0$. The reason for this is

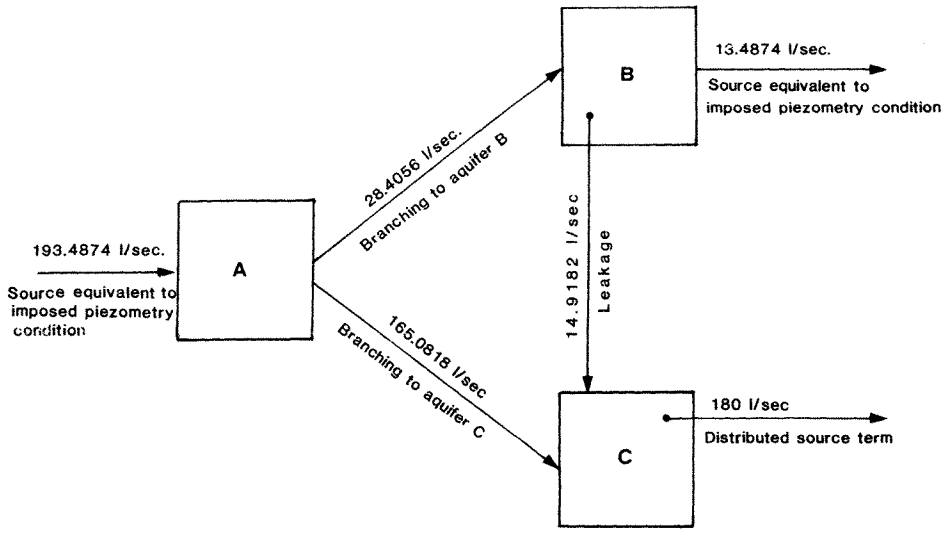

Figure 13. Fluid mass balance along three aquifers of the Figure 10 system

Table I. Comparison between method E.N.S. and the conventional method for the evaluation of fluid mass balance in the steady-state (The balance terms are expressed in l/s)

		Coarse-grid with 60 m sides		Fine-grid with 12 m sides	
	Theoretical value	Conventional method	E.N.S.	Conventional method	E.N.S.
Source equivalent to imposed piezometry conditions Aquifer A $y = 0$	193·4874	193·5829	193·5832	193·4437	193·4444
Flow entering Aquifer B through branching lines $y = 120$	28·4056	27·4560	28·1878	28·4223	28·4579
Flow entering Aquifer C through branching lines $y = 120$	165·0818	136·1256	165·3935	159·0140	164·9793
Source equivalent to imposed piezometry conditions Aquifer B $y = 300$	13·4874	17·0531	13·5819	14·1694	13·4638

that the elements affected by the imposed piezometry conditions are without any source and leakage terms, and that the case is steady state. In this case, (34) is reduced to the term $\sum_s a_{ms} h_s$ which expresses the source term evaluation, only on the basis of the shape function derivative, in a manner very similar to the conventional one. In the presence of source terms, leakage terms and storage depletion (for the unsteady case), the conventional method assigns as flow crossing an aquifer section, even the fluid mass which in reality participates as a source term, leakage term or storage depletion on the elements in contact with the section line. The mass, improperly assigned as mass flowing through the aquifer section, is the one that pertains to the node of the section line, in the partition of the element's fluid mass into nodal terms. This fact is evident if the flow exiting through the extreme $y = 300$ of aquifer C (Figure 11), is evaluated with the conventional method. Instead of a null flux, coherently with the posed boundary condition, an exiting flux is revealed equal to 26·5278 l/s. This flux is equal to approximately one half of the source terms pertinent to the four interested elements and can be estimated as 60 l/s, which decreases for 6·818 l/s due to leakage (evaluated on the basis of finite elements solution).

The difference between the conventional method and that E.N.S. increases as much as the source term increases (and storage depletion in the unsteady case). This fact is illustrated in Table I.

In the examined case, the major difference between the two methods occurs in the evaluation of the flux entering Aquifer C through the branching lines. This is due to the fact that the meshes of the third substructure in contact with the branching line are affected by the distributed source term (in addition to leakage). On the other hand, a minor difference is noted in the evaluation of flux entering Aquifer B through the branching line. This is due to the fact that this aquifer is affected only by leakage (less important than the distributed source term). Equation (34) can be considered different from the conventional formulation for two corrective terms. The first $\sum C_{ms} \dot{h}_s$ tied to storage depletion, and the second $-b_m$, tied to the source term present on the elements in contact with the line in question. The relative

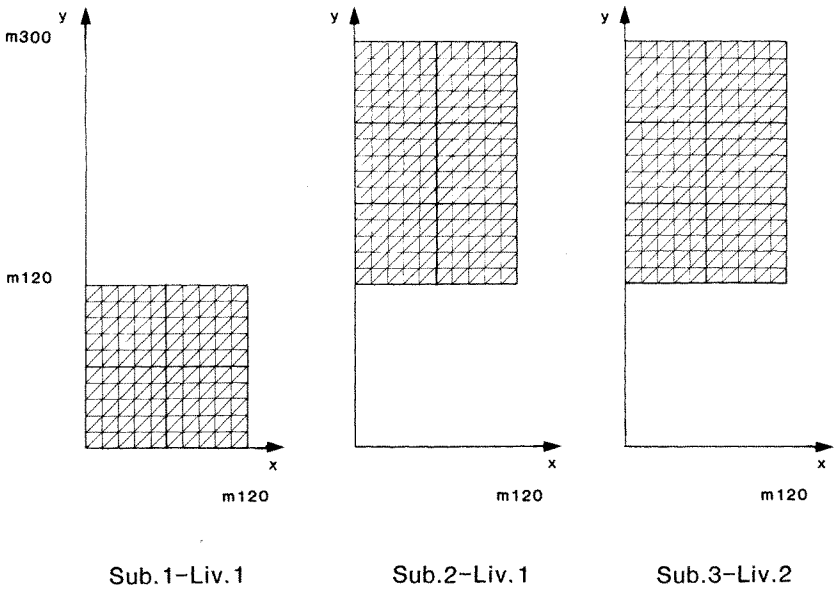

Figure 14. Schematization by finite elements with three substructures of the interconnected aquifer system of Figure 10. Fine network (800 aquifer elements, 165 aquitard macroelements, 462 nodes)

importance of these two corrective terms tends to decrease with the decrease in the mesh area. Hence, by thickening the network, the two methods tend to give the same results (this is not the case for meshes affected by punctual source terms). This is evident in Table I, which also indicates the calculation of finite elements related to the same case with network whose side elements are five times less, as illustrated in Figure 14 (fine network).

The comparison between the two cases, and between these and the analytical solution, points out how on the whole, the E.N.S. method provides a degree of accuracy for the coarse network (32 aquifer elements, 9 aquitard macroelements, 27 nodes), which is similar to that of the conventional method on the fine network (800 aquifer elements, 165 aquitard macroelements, 462 nodes). In some situations the conventional method gives better results (evaluation of flow entering Aquifer B through the branching line, with the fine network); and this can occur in cases in which both methods give good results and the difference between the two evaluations is insignificant.

The rectangular monolayered aquifer illustrated in Figure 15, was used to verify the

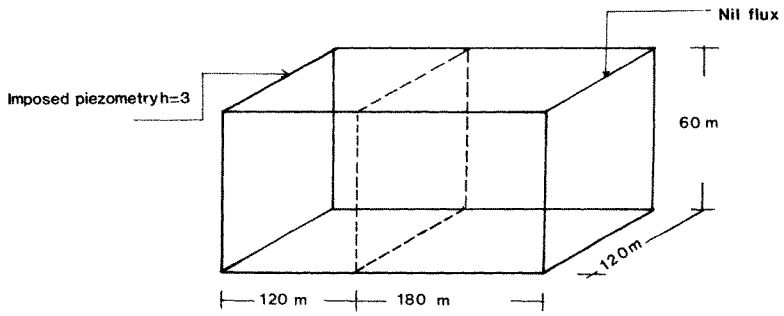

Figure 15. Monolayered aquifer for verification of the unsteady-state case

Table II. Timestep advancement scheme for the unsteady calculation on the monolayered aquifer of Figure 15

Macrostep number	No. of steps	Length of time (s)
1	15	5
2	1	75
3	3	150
4	3	300
5	2	750
6	2	1500
7	3	3000
8	1	7500

unsteady case. The initial conditions and the constants were considered uniform and the boundary conditions are such as to have the one-dimensional case. The solution to this problem was given by Carslaw and Jaeger;[7]

$$h(y, t) = h_0 - \frac{4h_0}{\pi} \sum_{0}^{\infty} \frac{(-1)^n}{2n+1} \exp\left\{-\frac{T(2n+1)^2\pi^2}{S4L^2} t\right\} \tag{99}$$

where $h_0 = 3$ m, $L = 300$ m, $T = 0{\cdot}06$, $S = 0{\cdot}01$

For the finite elements solutions, two finite element networks were considered. The first coarse network with a 60 m cathetus, as in the case of Figure 11, and the second fine network, with a 12 m cathetus, as in Figure 14, with only the first level considered. For both networks, the elaborations in unsteady state were carried out with the timestep advancement scheme of Table II.

Table III. Flow equivalent to imposed piezometry conditions ($h = 3$ for $y = 0$) for the unsteady case of Figure 15. Comparison between E.N.S. method and the conventional method

		Coarse-grid case sides = 60 m		Fine-grid case sides = 12 m	
t (s)	Analytical values of flux	E.N.S.	Conventional method	E.N.S.	Conventional method
75	574·4776	486·2936	364·8035	580·8455	565·4665
150	406·2166	388·1024	307·2692	400·6765	391·3926
300	287·2385	286·9465	242·5837	283·6804	280·7322
450	234·5293	231·4578	208·1661	231·6287	230·2854
600	203·1083	200·6151	185·1792	202·5429	201·7849
900	165·8372	165·1372	155·0811	164·2884	163·7827
1 200	143·6182	142·6315	136·4231	143·2759	143·0000
1 500	128·4453	127·6193	123·2347	127·7376	127·5326
2 250	104·6177	104·2376	101·3232	104·0906	103·9660
3 000	89·6087	89·4018	87·5725	88·9699	88·8906
4 500	68·8734	68·8700	67·5360	68·7755	68·7234
6 000	53·6899	53·6469	52·6571	53·3568	53·3175
9 000	32·7656	32·3734	31·6773	32·5624	32·5367
12 000	20·0032	19·4802	19·0609	19·3683	19·3532
15 000	12·2119	11·7191	11·4659	12·0159	12·0080
22 500	3·5563	2·7915	2·6753	2·6137	2·6098

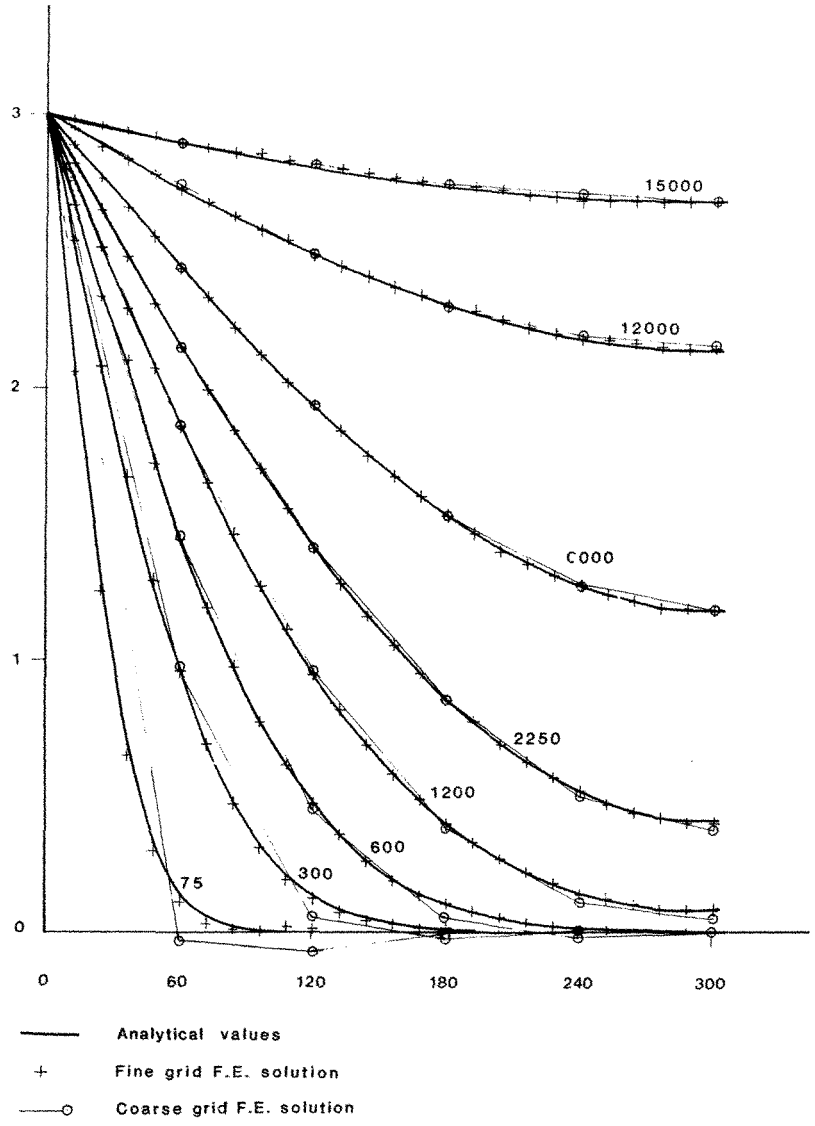

Figure 16. Piezometric trend for the unsteady-state case on the monolayered rectangular aquifer (120 m × 300 m × 60 m) of Figure 15

Figure 16 illustrates the analytical solution and the solution of finite elements along the middle section with the two adopted networks.

Table III illustrates in time, the flow equivalent to the imposed piezometry conditions for $y = 0$, and Table IV indicates the flow crossing the section $y = 120$ m. The evaluation is made both with the previously illustrated conventional method, and with the E.N.S. method. Both methods are compared with the analytical values, inferred by applying Darcy's law to the piezometry expressed with (99). On the basis of both tables, it results that, even for the unsteady case, the E.N.S. method applied with the coarse network (20 elements and 18 nodes), has a precision comparable to that of the conventional method on the fine network

Table IV. Flow evaluated through section $y = 120$ of the unsteady case of Figure 15. Comparison between the E.N.S. method and the conventional method

		Coarse-grid case sides = 60 m		Fine-grid case sides = 12 m	
t (s)	Analytical values of flux	E.N.S.	Conventional method	E.N.S.	Conventional method
75	0·3469	−42·9251	−12·8005	−0·0209	0·0203
150	10·4161	5·3820	−14·0288	7·0194	3·7543
300	46·6481	42·5220	10·3418	39·3256	28·8406
450	70·0640	62·0124	33·1061	63·2973	54·9799
600	82·1912	75·4193	47·2575	74·8102	68·3094
900	90·8170	82·2895	62·4842	85·3812	80·6168
1 200	91·4264	85·5858	68·4060	86·8351	83·3456
1 500	89·3721	85·1001	70·3061	85·8633	82·7317
2 250	81·1537	76·9082	68·0113	78·5052	76·9463
3 000	72·3726	70·0648	61·5436	70·5675	68·9427
4 500	56·7988	54·6419	48·5171	55·2529	54·2682
6 000	44·4066	42·7269	37·6928	43·2364	42·2685
9 000	27·1127	25·2190	22·6893	25·9416	25·5917
12 000	16·5523	15·1742	13·6454	15·7499	15·4109
15 000	10·1052	9·1292	8·2123	9·4525	9·3658
22 500	2·9428	1·8493	1·9135	2·2287	2·1795

(500 elements, 286 nodes). In the case of Table III it should be pointed out how in some cases the E.N.S. method does not improve its accuracy (and in some cases it is worsened) in the fine network case. Nevertheless, it provides better results than the corresponding conventional case. This is explained by the fact that the corrective effect of the term $\sum C_{ms}\dot{h}_s$ decreases corresponding to the nearing of affected nodes (caused by the effect of mesh reduction) to boundary nodes, for which it is $\dot{h}_s = 0$, as an effect of the constant imposed piezometry conditions. The differences however are insignificant, and in any case the E.N.S. method gives better results than the conventional one. This does not occur in the case of Table IV concerning flow evaluation along section $y = 120$ m. The sudden transfer from the piezometry of value 0 to time $t = 0$, to value 3 to time $t = 0_+$ for the nodes subject to imposed piezometry conditions, creates a few problems to the Crank–Nicolson method for the initial times. This is the cause of the unnatural negative flows for 75 s and 150 s, estimated in section $y = 120$ both by means of the conventional method and the E.N.S. method. This effect, which concerns only the initial times, can be reduced by reducing the timestep and the newtork's mesh. Figure 16 illustrates the finite element solution compared with the corresponding analytical solution. Figure 17, on the other hand, illustrates the comparison between the E.N.S. method for flux evaluation and the conventional one, for the two sections in question ($y = 0$ and $y = 120$), for the coarse grid case. The slight violations in the mass conservation of the E.N.S. method, which can be seen in Table I for the steady and unsteady case, are caused by the truncation error when assembling equations (34) and (37), and by the residual error in piezometry due to the iterative process. This violation is more relevant for the unsteady case since, in addition to the truncation error in assembly of (34) and (37) there is an error caused by the finite difference estimation of time derivative, and the error introduced by the predictor–corrector procedure. With the purpose of checking these errors, an indicator of balance quality is elaborated for each balance, formed by the quotient

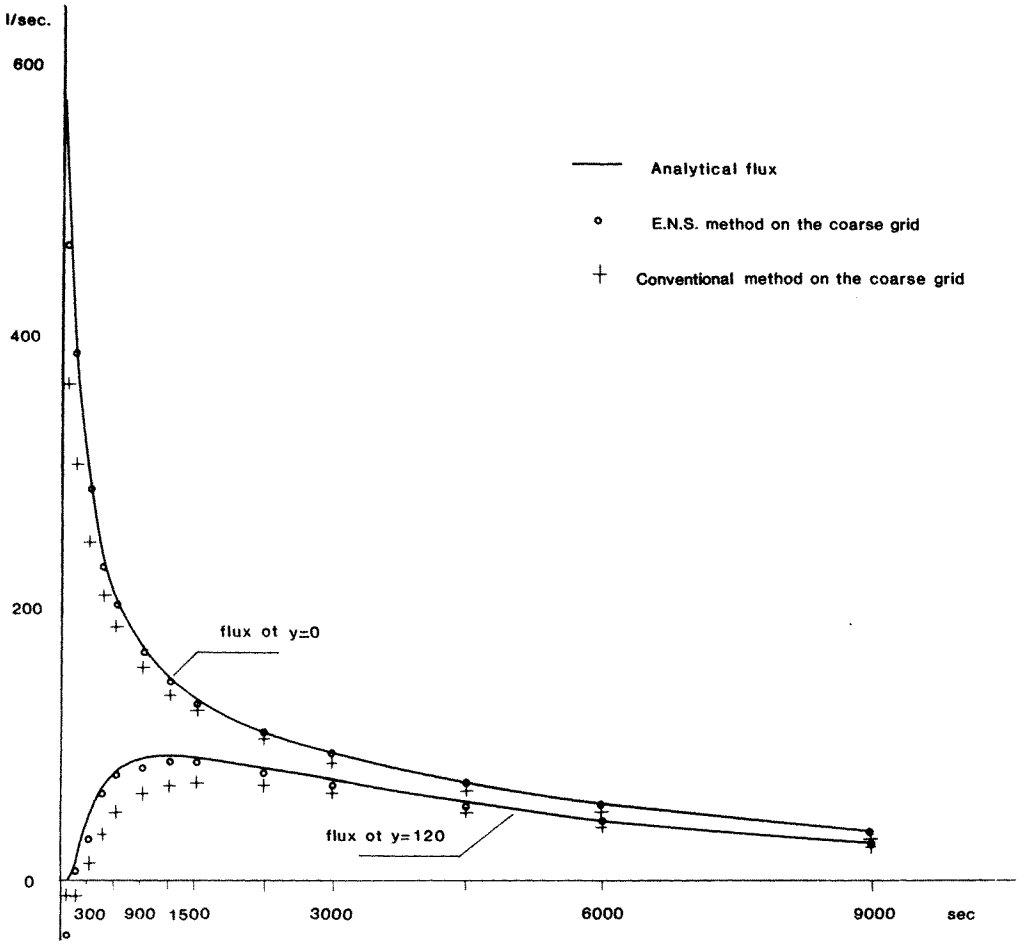

Figure 17. Flux evaluation in the unsteady-state regime along sections $y = 0$ and $y = 120$ of the monolayered rectangular aquifer. Comparison between E.N.S. method and the conventional method

between the difference of the computed mass entering and exiting from the zone interested by the balance, and the average of entering and exiting mass.

For the steady state case of Figure 10, the indicator resulted less 0·23 per cent for balance evaluation of the three substructures which form the aquifer. In the unsteady state case of Figure 15, the balance was estimated in the two substructures in which the aquifer is divided by section $y = 120$. The balance quality indicator assumed average values of approximately 3 per cent, reaching values of 10 per cent when the entering/exiting water masses resulted a small quantity when approaching the steady state regime (about 0·01 l/s). No significant differences were recorded between the coarse-grid and fine-grid network, in relation to the balance quality indicator.

The illustrated method has been applied in very complex practical cases. The operational performance met the expectations. Particularly, it was confirmed that the trend of time consumption of C.P.U. according to the degree of freedom of the system is typical of bidimensional cases, and not the most onerous one of three-dimensional problems, to which the problem is comparable in relation to the structure of the matrix of system (19). In the

Table V. Description of three applications

Cases	I	II	III
Number of aquifer levels	2	2	3
Number of substructures	4	12	20
Number of elements on aquifers	693	3529	4407
Number of aquitard macroelements	109	312	776
Number of elements per macroelement	4	4	4
Total number of elements	1129	4777	7511
Number of nodes on aquifers	419	1917	2362
Number of aquitard internal nodes	327	936	2328
Total number of nodes	746	2853	4690
Number of branching nodes	10	41	62
Average linear front		53·21	48·58
Average quadratic front		64·55	58·93
Maximum front		145	139

I Case: Coarse network used for preliminary calibration of two layered mathematical model of Western Libya aquifer.
II Case: Fine network for two layered mathematical model of the same aquifer.
III Case: Fine network for three layered detailed model of Western Libya aquifer.

Table VI. C.P.U. times and iterations of the steady state case

Cases	I	II	III
C.P.U. times (s) on IBM 3033	30·83	172·46	259·21
Number of iterations	3	6	6
Dominating eigenvalues of $\mathbf{P}$		−2·2	−2·4
Dominating eigenvalue of $\bar{\mathbf{P}}$		0·14	0·45

Table VII. C.P.U. times and timesteps for the unsteady case

Cases	I	II	III
Simulation period	8 040 BC	1 979	1 980
	1 960	2 050	2 030
Duration of simulation (years)	10 000	71	50
Number of macrosteps	2	2	2
Total number of steps	19	15	24
Step duration 1st macrostep (years)	100	3	1·25
Number of steps 1st macrostep	10	2	8
Step duration 2nd macrostep (years)	1 000	5	2·5
Number of steps 2nd macrostep	9	13	16
C.P.U. time (s) on IBM 3033	151	780	1147

The models cover a total surface of 800 000 km^2
The minimum area element in the 2nd and 3rd case has a surface of 3 km^2
The maximum area is approximately 3 000 km^2

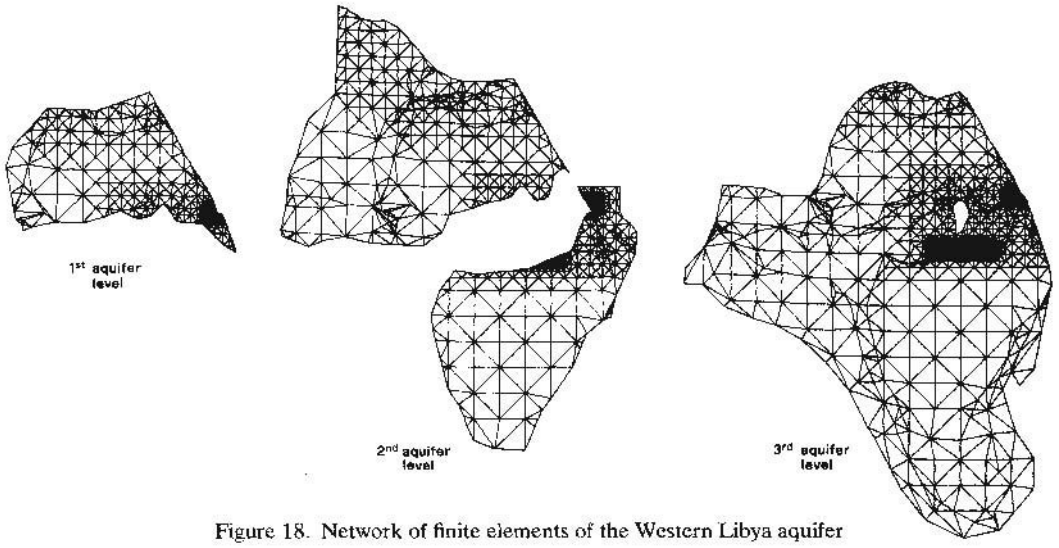

Figure 18. Network of finite elements of the Western Libya aquifer

steady-state case there has been a rapid convergence of the iterative method (a maximum of 7 iterations for the most complex cases). In the unsteady cases, the predictor–corrector method proved to be very stable, and this permitted the use of very wide timesteps. In particular, a simulation was carried out along a time span of 10,000 years (simulation of the aquifer trend in Western Libya from the last pluvial age to the present).

Table V illustrates 3 real particularly significant cases.

Table VI gives the C.P.U. time employed in the steady state case, indicating the number of iterations requested and the estimate of dominating eigenvalues of matrix $\mathbf{P}$ and $\bar{\mathbf{P}}$ related to this case. The iterative process is stopped when the mean quadratic residual between 2 iterations is less than one centimetre.

Table VII illustrates the timesteps characteristics and the C.P.U. time for the unsteady case.

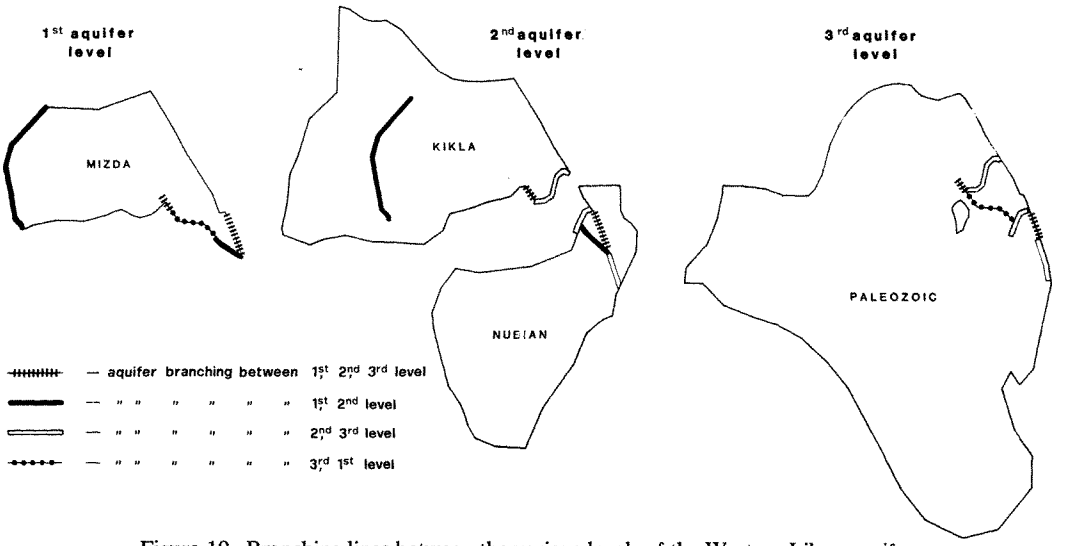

Figure 19. Branching lines between the various levels of the Western Libya aquifer

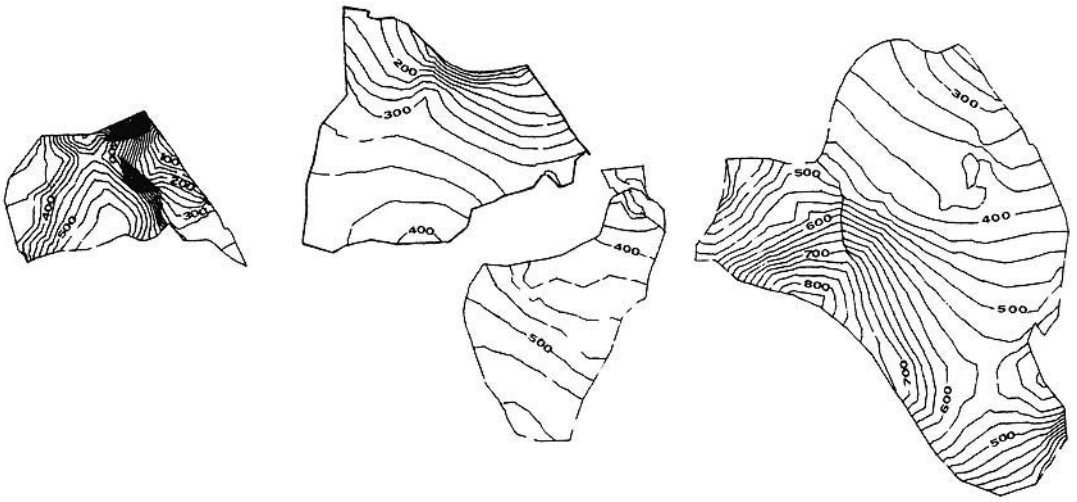

Figure 20. Piezometric distribution in the year 1960 reproduced by the model

Figure 18 represents the network of finite elements of the III case, whereas the II case has a network composed only of 2nd and 3rd level elements in the III case. Figure 19 illustrates the branching lines of the III case.

Typical results given by the model are presented in Figures 20 and 21. Figure 20 represents the steady state piezometric distribution given by the model and corresponds to the groundwater system prior to its modern development (year 1960); Figure 21 shows the groundwater past history in the Al Jufrah area. In this area only the Mizda Aquifer is exploited. The piezometric decline observed in the Paleozoic aquifer is due to the combined effect of the leakage through the Cenomanian Aquitard and of the lateral contact between the Mizda and the Paleozoic Aquifers along the Aquifer branching SE of Al Jufrah in

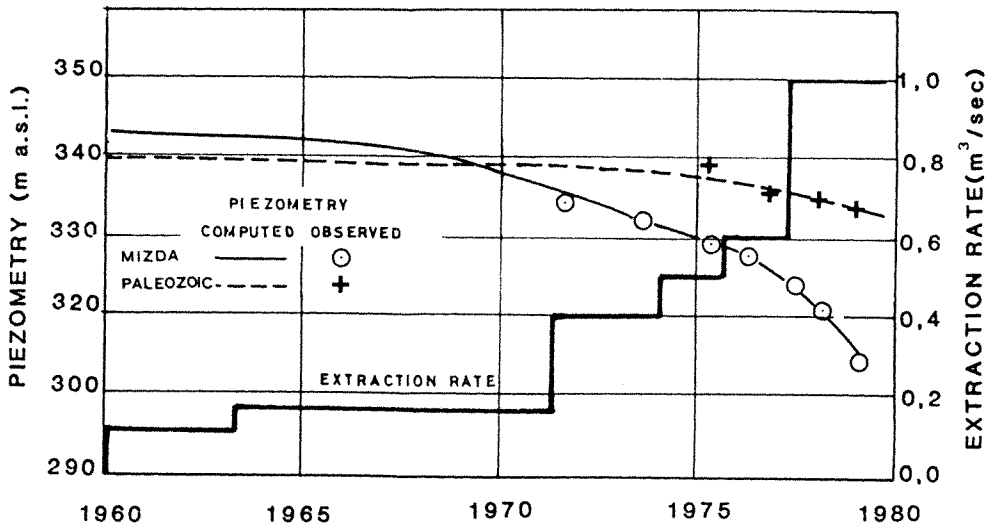

Figure 21. Groundwater production history in Al Jufrah

correspondance of the physical boundary of the Cenomanian aquitard. More details about the Western Libya aquifer model are given by Pizzi and Sartori.[8]

ACKNOWLEDGEMENTS

The authors wish to thank Mr. J. Donea and Mr. S. Giuliani of the Joint Research Center Ispra Establishement, and Mr. G. Pizzi of Aquater S.p.A. in San Lorenzo in Campo (PS) for their critical contributions and suggestions.

This methodology was applied in the 'Hydrogeological Study of Wadi Ash Shati, Al Jufrah and Jabal Fezzan Area' carried out by Aquater (Idrotecneco)[9] for the Secretariat of Agricultural Reclamation and Land Development, Department of Water and Soil, of the Socialist People's Libyan Arab Jamahiriya.

Thanks are due to O. Jarroud, A. Mandour, P. Pallas, A. El Sunni, A. Zafar of the Water and Soil Department, for their contribution to the work.

We also wish to express our sincere thanks to Mrs. L. Fontana and Miss M. Paci for their editing and typing contribution, to Mrs. E. Gasparini for graphic reproductions and Mrs. P. Lorenzetti for the English translations.

REFERENCES

1. S. P. Neuman and P. A. Witherspoon. 'Theory of flow in a confined two-aquifer system', *Water Resources Research*, **5,** 817 (1969).
2. K. Fujinawa, 'Finite element analysis of groundwater flow in multiaquifer systems, I. The behavior of hydrogeological properties in an aquitard while being pumped', *Journal of Hydrology*, **33,** 59–72 (1977).
3. K. Fujinawa. 'Finite element analysis of groundwater flow in multiaquifer systems, II. 'A quasi three-dimensional flow model', *Journal of Hydrology*, **33,** 349–362 (1977).
4. Don W. Chorley and Emil O. Frind, 'An iterative quasi-three dimensional finite element model for heterogeneous multiaquifer systems', *Water Resources Research*, **14** (5), 943–952 (1978).
5. B. M. Irons. 'A frontal solution program for finite element analysis', *International Journal for Numerical Methods in Engineering*, **2,** 5–32, (1970).
6. Jan N. Smith, 'Integration in time of diffusion and diffusion–convection equations', *1st Int. Conf. on Finite Elements in Water Resources*, Princeton, 1976.
7. H. S. Carslaw and J. C. Jaeger, *Conduction of Heat in Solids*, Oxford University Press, 1978.
8. G. Pizzi and L. Sartori, 'Interconnected Groundwater System Simulations (IGROSS). Description of the system and its applications to the Western Libya regional aquifer', *4th Int. Conf. on Finite Elements in Water Resources*, Hannover, 1982.
9. Aquater (Idrotecneco), *Hydrogeological Study of Wadi Ash Shati, Al Jufrah and Jabal Fezzan area.* Prepared for Secretariat of Agricultural Reclamation and Land Development. Tripoli, Libya, 1981.
10. J. J. Connor and C. A. Brebbia, *Finite Element Techniques for Fluid Flow*, Newnes-Butterworths, London, 1977.
11. J. H. Edelman, *Groundwater Hydraulics of Extensive Aquifers*, International Institute for Land Reclamation and Improvement, Wageningen, 1972.
12. L. Sartori and G. Peverieri, 'A frontal method based solution of the quasi-three-dimensional finite element model for interconnected aquifer systems and fluid mass balance evaluation. Steady and unsteady equations', *4th Int. Conf. on Finite Elements in Water Resources*, Hannover, 1982.